Electronic Supplementary Material (ESI) for ChemComm.
This journal is © The Royal Society of Chemistry 2021

Electronic Supplementary Information

Light-controlled interconversion between a [*c2*]daisy chain and a lasso-type pseudo[1]rotaxane

Chih-Wei Chu, Daniel L. Stares and Christoph A. Schalley*

Institut für Chemie und Biochemie, Organische Chemie, Freie Universität Berlin, Arnimallee 20, 14195 Berlin, Germany

Table of contents

1. General information

All reagents and solvents were purchased from commercial sources and used without further purification. Dry solvents were purchased from Acros Organics in sealed containers. Precursors **S1**,[S1, S2] **S2**,[S3] **S5**[S4] and **S7**[S5] were synthesised according to reported procedures. Thin-layer chromatography was performed on silica gel-coated plates with fluorescent indicator F254 (Merck). For column chromatography, silica gel (0.04-0.063 mm; Merck) was used.

^{1}H and ^{13}C NMR experiments were recorded on JEOL ECX 400, JEOL ECP 500, Bruker AVANCE 500 or Bruker AVANCE 700 instruments. Solvent residue signals were used as the internal standard. All shifts are reported in ppm and NMR multiplicities are abbreviated as s (singlet), d (doublet), t (triplet), q (quartet), quint (quintet), sext (sextet), m (multiplet) and br (broad). Coupling constants *J* are reported in Hertz.

UV/vis spectra were recorded on a Varian Cary 50 Bio spectrometer with a xenon lamp. Compounds were dissolved in HPLC grade solvents. Suprasil glass cuvettes with path-lengths of 1 cm or 0.1 cm were used.

Two different light sources were used in photoswitching experiments (both NMR and UV/vis). A UV hand lamp from Herolab GmbH with a 6 W tube at 365 nm was used for *E*-*Z*-isomerisation. A Thorlabs M530L4 LED with a LED current of 1000 mA was used for *Z*-*E*-isomerisation. In experiments to determine the PSS, irradiation time was 15 min in both directions.

High-resolution ESI mass spectra were measured on an Agilent 6210 ESI-TOF instrument. Travelling-wave ion-mobility spectrometry mass spectrometry (IMS-MS) and collision-induced dissociation (CID) experiments were performed on a Synapt G2-S HDMS Q-TOF (Waters Co., Milford, MA, USA) instrument equipped with a Z-spray electrospray ionisation (ESI) ionisation source. A sample concentration of 10 µM in DCM was used for measurements with a flow rate of 5 µL/min. A capillary voltage of 2 kV was used with sample cone and source offset both set to 15 V. Source and desolvation temperature were set to 40 ºC. IMS and CID measurements were both performed with N_2. IMS measurements used the following settings: trap gas flow 0.40 mL/min, helium cell gas flow 180 mL/min; IMS gas flow 120 mL/min; wave height 32 V; wave velocity 550 m/s. The instrument was allowed to settle for 45 minutes prior to data acquisition. IMS measurements were done for the mass-selected ion at *m/z*

654. Arrival-time distributions (ATDs) are presented in milliseconds.

Computational calculations were performed using the semi-empirical PM6 method in the program Scigress (Fujitsu, version FJ 2.9.1).

Theoretical collisional cross section calculations (CCS) in nitrogen buffer gas ($^{TM}CCS_{N_2}$) were calculated using the trajectory method using the IMoS parallelised tool set. (https://doi.org/10.1007/s13361-017-1661-8)

2. Synthesis of thread 1 and control compound 2

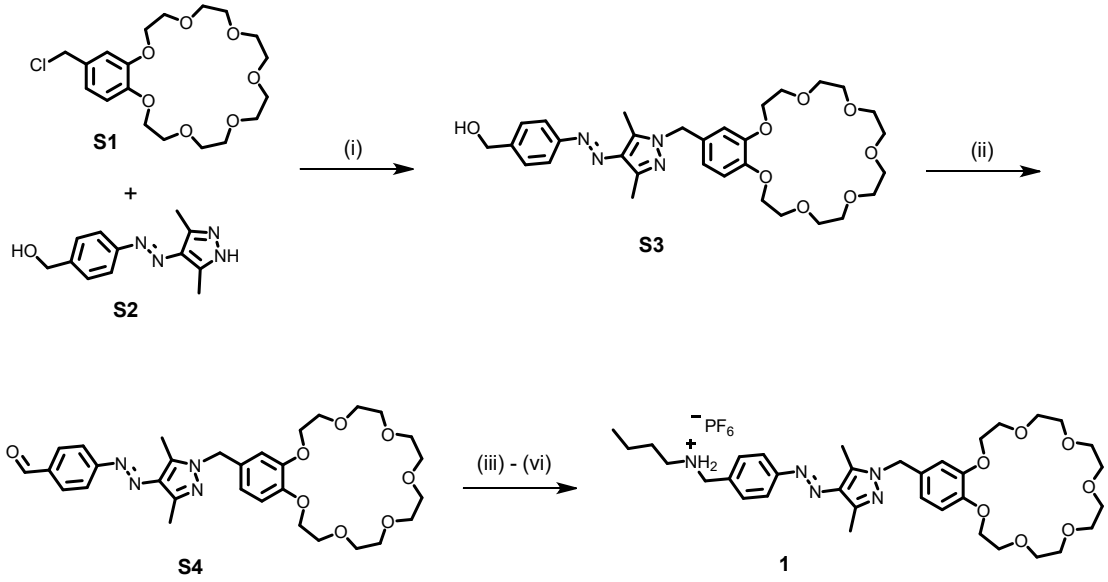

Scheme S1. Synthesis procedures for thread **1**. Reaction conditions: (i) K_2CO_3, dry ACN, reflux; (ii) Dess-Martin periodinane, dry DCM, 0 ºC; (iii) *n*-butylamine, EtOH, reflux; (iv) $NaBH_4$, EtOH, 0 ºC; (v) HCl, MeOH; (vi) NH_4PF_6 (aq).

Synthesis of S3

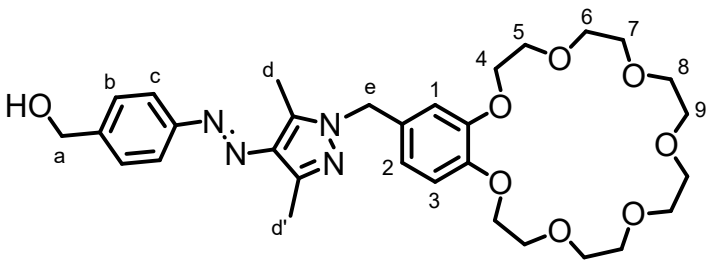

Compound **S2** (230 mg, 1.00 mmol, 1.00 eq.) and K_2CO_3 (690 mg, 5.00 mmol, 5 eq) were added to a solution of **S1** (414 mg, 1.00 mmol, 1.00 eq.) in dry ACN (30 mL) under argon atmosphere. This mixture was stirred at reflux for 4 days. After rotary evaporation, the residue was dissolved in CH_2Cl_2 (100 mL). The organic phase was washed with 1 M HCl (1×100 mL) and brine (2×100 mL), before it was dried over $MgSO_4$ and concentrated by rotary evaporation. Further purification was carried out by column chromatography on silica gel (CH_2Cl_2/MeOH = 94:6), yielding the title compound as viscous orange oil (468 mg, 78%, R_f ~ 0.3).

^{1}H NMR (500 MHz, $CDCl_3$, 298 K): δ = 7.79-7.74 (m, H_c, 2H), 7.47-7.42 (m, H_b, 2H),

6.84-6.79 (m, H_1 and H_3, 2H), 6.75-670 (m, H_2, 1H), 5.24 (s, H_e, 2H), 4.75 (s, H_a, 2H), 4.14-4.10 (m, H_4, 4H), 3.91-3.87 (m, H_5, 4H), 3.79-3.75 (m, H_6, 4H), 3.73-3.69 (m, H_7, 4H), 3.67-3.61 (m, H_8 and H_9, 8H), 2.56 (s, H_d, 3H), 2.54 (s, $H_{d'}$, 3H) ppm.

^{13}C NMR (126 MHz, $CDCl_3$, 298 K): δ = 153.12, 149.37, 148.89, 142.61, 142.39, 139.31, 135.46, 129.00, 127.57, 122.19, 120.28, 114.34, 113.47, 71.22, 71.20, 71.19, 71.14, 71.12, 70.68, 69.84, 69.42, 65.08, 52.92, 13.84, 10.22 ppm.
ESI-MS (*m*/*z*): calculated for $[C_{31}H_{42}N_4O_8Na]^+$: 621.2895, found 621.2899.

Synthesis of S4

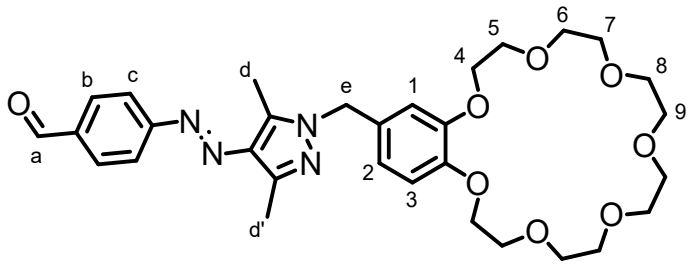

Compound **S3** (263 mg, 0.44 mmol, 1.00 eq.) in dry CH_2Cl_2 was added dropwise to a solution of Dess-Martin periodinane (280 mg, 0.65 mmol, 1.50 eq.) in dry CH_2Cl_2 (10 mL) under argon atmosphere at 0 ºC. This mixture was stirred at this temperature for 1 h and then at room temperature for additional 2 h. Afterwards, the mixture was diluted with CH_2Cl_2 (50 mL). The organic phase was washed with saturated $NaHCO_3$ (1×50 mL) and brine (1×100 mL), before it was dried over $MgSO_4$ and concentrated by rotary evaporation. Further purification was carried out by column chromatography on silica gel (CH_2Cl_2/MeOH = 97:3), yielding the title compound as viscous orange oil (200 mg, 76%, R_f ~ 0.20).

^{1}H NMR (700 MHz, $CDCl_3$, 298 K): δ = 10.06 (s, H_a, 1H), 7.98-7.96 (m, H_b, 2H), 7.90-7.87 (m, H_c, 2H), 6.83 (d, *J* = 8.2 Hz, H_3, 1H), 6.76 (d, *J* = 2.1 Hz, H_1, 1H), 6.72 (dd, *J* = 8.2, 2.1 Hz, H_2, 1H), 5.20 (s, H_e, 2H), 4.15-4.10 (m, H_4, 4H), 3.91-3.88 (m, H_5, 4H), 3.79-3.75 (m, H_6, 4H), 3.73-3.69 (m, H_7, 4H), 3.67-3.64 (m, H_8 and H_9, 8H), 2.54 (s, H_d and $H_{d'}$, 6H) ppm.

^{13}C NMR (176 MHz, $CDCl_3$, 298 K): δ = 191.85, 157.38, 149.40, 148.94, 143.07, 140.43, 136.74, 133.57, 131.99, 130.83, 129.14, 122.44, 120.10, 114.39, 113.47,

71.25, 71.17, 70.70, 69.85, 69.56, 69.48, 53.17, 14.32, 10.28 ppm.

ESI-MS (*m*/*z*): calculated for $[C_{31}H_{10}N_4O_8Na]^+$: 619.2738, found 619.2743.

Synthesis of 1

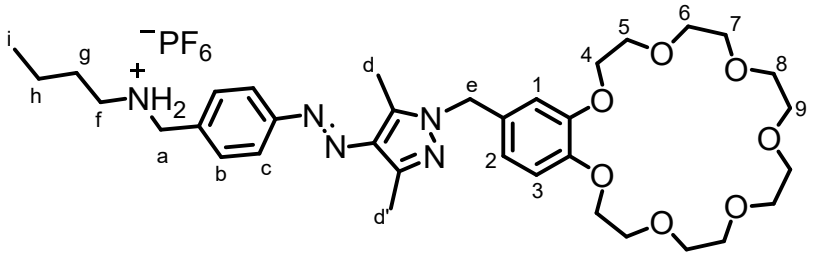

n-Butylamine (37 µL, 0.37 mmol, 1.10 eq.) was added dropwise to a solution of **S4** (200 mg, 0.34 mmol, 1.00 eq.) in dry EtOH (10 mL) under argon atmosphere at room temperature. This mixture was heated to reflux and stirred at 95 ºC overnight. Afterwards, the mixture was cooled down to 0 ºC, and sodium borohydride (39 mg, 1.02 mmol, 3.00 eq.) was added slowly. The suspension was stirred at 0 ºC for 1 h and then at room temperature overnight. The mixture was quenched by adding 1 mL of saturated $NaHCO_3$ and concentrated under reduced pressure. The residue was dissolved in CH_2Cl_2 (50 mL) and extracted with brine (3×50 mL). The organic phase was dried over $MgSO_4$ and concentrated by rotary evaporation. The amine was dissolved in MeOH (5 mL) and concentrated HCl (0.5 mL) was added. The mixture was stirred at room temperature for 15 minutes before 10 mL of water was added. To this solution, 1 mL of NH_4PF_6 solution (100 mg/mL) was added to precipitate the product. After stirring for 30 minutes, the precipitate was collected by vacuum filtration, washed with water and dried in a vacuum oven. The title compound was obtained as a yellow solid. (139 mg, 63% over three steps).

^{1}H NMR (700 MHz, DMSO-d_6, 298 K): δ = 8.71 (s, NH_2-, 2H), 7.79 (d, *J* = 8.3 Hz, H_b, 2H), 7.62 (d, *J* = 7.5 Hz, H_c, 2H), 6.92 (d, *J* = 8.3 Hz, H_3, 1H), 6.90 (d, *J* = 1.4 Hz, H_1, 1H), 6.70 (dd, H_2, *J* = 8.3 and 1.4 Hz, 1H), 5.24 (s, H_e, 2H), 4.21 (s, H_a, 2H), 4.08-4.03 (m, H_4, 4H), 3.76-3.71 (m, H_5, 4H), 3.61-3.57 (m, H_6, 4H), 3.56-3.52 (m, H_7, 4H), 3.52-3.47 (m, H_8 and H_9, 8H), 2.96-2.91 (t, *J* = 6.9 Hz, H_f, 2H), 2.56 (s, H_d, 3H), 2.41 (s, $H_{d'}$, 3H), 1.63-1.57 (quin, *J* = 7.7 Hz, H_g, 2H), 1.37-1.31 (sext, *J* = 7.5 Hz, H_h, 2H), 0.9 (t, *J* = 7.4 Hz, H_i, 1H) ppm.

^{13}C NMR (176 MHz, DMSO-d_6, 298 K): δ = 153.19, 148.07, 147.73, 140.85, 139.94,

134.73, 133.04, 130.84, 129.16, 121.59, 119.82, 113.45, 113.02, 70.24, 70.22, 70.14, 69.87, 68.89, 68.41, 68.31, 51.92, 49.66, 46.42, 27.42, 19.25, 13.95, 13.47, 9.61 ppm. **ESI-MS** (*m*/*z*): calculated for $[C_{35}H_{51}N_5O_7K]^+$: 692.3420, found 692.3415.

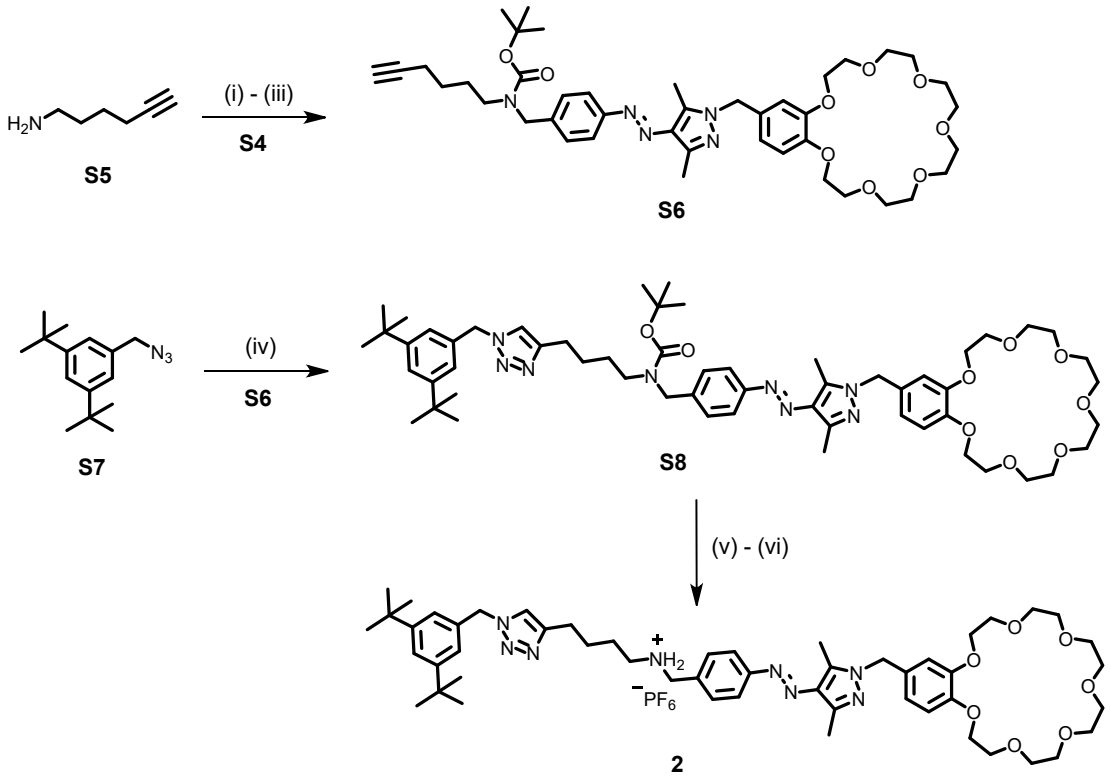

Scheme S2. Synthesis procedures for control compound **2**. Reaction conditions: (i) **S4**, dry THF, reflux; (ii) $NaBH_4$, THF, 0 ºC; (iii) Boc_2O, Et_3N, DCM; (iv) **S6**, $Cu(ACN)_4PF_6$, tris(benzyltriazolylmethyl)amine (TBTA), DCE, 45 ºC; (v) HCl, MeOH; (vi) $NH_4PF_{6(aq)}$.

Synthesis of S6

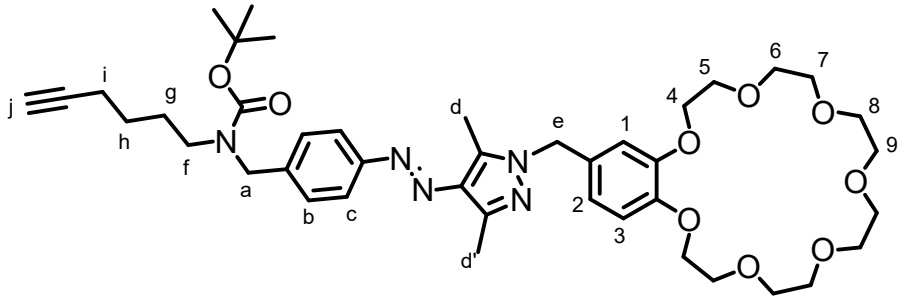

5-Hexynyl-1-amine (12 mg, 0.13 mmol, 1.50 eq.) was added dropwise to a solution of **S4** (50 mg, 0.084 mmol, 1.00 eq.) in dry THF (6 mL) under nitrogen atmosphere at

room temperature. This mixture was heated to reflux and stirred at 80 ºC overnight. Afterwards, the mixture was cooled down to 0 ºC, and sodium borohydride (10 mg, 0.25 mmol, 3.00 eq.) was added slowly. The suspension was stirred at 0 ºC for 1 h and then at room temperature overnight. The mixture was quenched by adding 1 mL of saturated $NaHCO_3$ and concentrated under reduced pressure. The residue was dissolved in CH_2Cl_2 (50 mL) and extracted with 1 M NaOH (1×50 mL) and brine (1×50 mL). The organic phase was dried over $MgSO_4$ and concentrated by rotary evaporation. The amine was dissolved in dry DCM (10 mL) under nitrogen atmosphere, and di-*tert*-butyl dicarbonate (57 mg, 0.25 mmol, 3.00 eq.) and Et_3N (36 µL, 0.17 mmol, 2.00 eq.) were added subsequently. The mixture was stirred at room temperature overnight before extracting with 0.1 M HCl (1×30 mL), saturated $NaHCO_3$ (1×30 mL) and brine (1×30 mL). The organic phase was dried over $MgSO_4$ and concentrated by rotary evaporation. Further purification was carried out by column chromatography on silica gel (CH_2Cl_2/MeOH = 96:4), yielding the title compound as a yellow solid (33 mg, 51% over three steps, R_f ~ 0.30).

^{1}H NMR (700 MHz, $CDCl_3$, 298 K): δ = 7.73 (d, *J* = 8.0 Hz, H_b, 2H), 7.30 (m, H_c, 2H), 6.82 (d, *J* = 8.2 Hz, H_3, 1H), 6.74 (d, *J* = 2.1 Hz, H_1, 1H), 6.70 (dd, *J* = 8.2 and 2.1 Hz, H_2, 1H), 5.19 (s, H_e, 2H), 4.52-4.42 (m, H_a, 2H), 4.15-4.09 (m, H_4, 4H), 3.92-3.86 (m, H_5, 4H), 3.80-3.75 (m, H_6, 4H), 3.73-3.69 (m, H_7, 4H), 3.68-3.63 (m, H_8 and H_9, 8H), 3.29-3.12 (m, H_f, 2H), 2.52 (s, H_d, 3H), 2.51 (s, $H_{d'}$, 3H), 2.21-2.16 (m, H_i, 2H), 1.93 (t, *J* = 2.6 Hz, H_j, 1H), 1.52 (s, H_{Boc}, 9H), 1.51-1.40 (m, H_g and H_h, 4H) ppm.

^{13}C NMR (176 MHz, $CDCl_3$, 298 K): δ = 152.99, 149.34, 148.78, 146.88, 142.69, 139.01, 135.63, 129.47, 128.43, 127.72, 122.04, 120.09, 114.36, 113.31, 85.31, 79.92, 71.21, 71.14, 70.68, 69.84, 69.46, 68.68, 53.02, 29.84, 28.58, 27.56, 25.81, 18.29, 14.15, 10.20 ppm.

ESI-MS (*m*/*z*): calculated for $[C_{42}H_{59}N_5O_9Na]^+$: 800.4205, found 800.4201.

Synthesis of S8

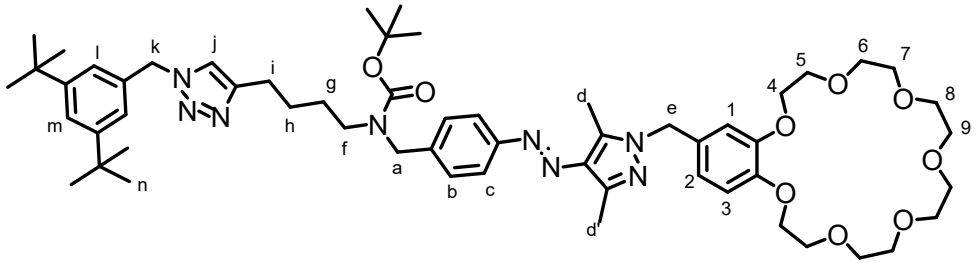

3,5-di-*tert*-butylbenzyl azide **S7** (36 mg, 0.147 mmol, 2.00 eq.) was added to a solution of **S6** (57 mg, 0.073 mmol, 1.00 eq.) in dry DCE (5 mL) under nitrogen atmosphere at room temperature. A stream of nitrogen gas was bubbled through this mixture for 15 minutes. Afterwards, tris(benzyltriazolylmethyl)amine (39 mg, 0.073 mmol, 1.00 eq.) and $Cu(ACN)_4PF_6$ (55 mg, 0.147 mmol, 2.00 eq.) were added subsequently before stirring at 40 ºC for 3 days. The solution was extracted with saturated $NaHCO_3$ (2×50 mL) and brine (1×50 mL). The organic phase was dried over $MgSO_4$ and concentrated by rotary evaporation. Further purification was carried out by column chromatography on silica gel (CH_2Cl_2/MeOH = 95:5), yielding the title compound as a yellow solid (44 mg, 59%, R_f ~ 0.30).

^{1}H NMR (700 MHz, $CDCl_3$, 298 K): δ = 7.78 (s, H_j, 2H), 7.74-7.69 (m, H_b, 2H), 7.40 (t, *J* = 1.8 Hz, H_m, 1H), 7.32-7.27 (m, H_c, 2H), 7.07 (d, *J* = 1.7 Hz, H_l, 2H), 6.85 (d, *J* = 8.3 Hz, H_3, 1H), 6.77 (d, *J* = 2.0 Hz, H_1, 1H), 6.74 (dd, *J* = 8.3 and 2.0 Hz, H_2, 1H), 5.45, (s, H_k, 2H), 5.20 (s, H_e, 2H), 4.48-4.39 (m, H_a, 2H), 4.17-4.12 (m, H_4, 4H), 3.90-3.86 (m, H_5, 4H), 3.73-3.70 (m, H_6, 4H), 3.66-3.64 (m, H_7, 4H), 3.68-3.63 (m, H_8 and H_9, 8H), 3.28-3.13 (m, H_f, 2H), 2.73-2.63 (m, H_i, 2H), 2.52 (m, H_d and $H_{d'}$, 6H), 1.66-1.57 (m, H_h, 2H), 1.51-1.47 (s, H_g and H_{Boc}, 11H), 1.29 (s, H_n, 18H) ppm.

^{13}C NMR (176 MHz, $CDCl_3$, 298 K): δ = 152.93, 151.84, 148.67, 148.35, 148.03, 142.78, 139.12, 135.63, 134.25, 129.27, 128.91, 128.40, 128.24, 127.74, 122.75, 122.38, 122.03, 120.71, 79.87, 70.04, 69.71, 69.36, 68.55, 54.73, 52.83, 35.02, 31.53, 28.59, 26.88, 25.55, 14.19, 10.18 ppm.

ESI-MS (*m*/*z*): calculated for $[C_{57}H_{82}N_8O_9Na]^+$: 1045.6097, found 1045.6067.

Synthesis of 2

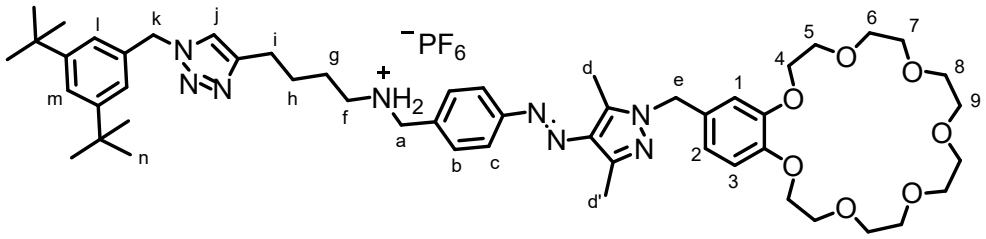

2 M HCl in diethyl ether (2 mL) was added dropwise to a solution of **S8** (31 mg, 0.03 mmol, 1.00 eq.) in DCM (2 mL) at 0 ºC. This mixture was stirred at this temperature for one hour and at room temperature for another one hour. Afterwards, the volatiles were removed by rotary evaporation and the residue was dissolved in

DCM (50 mL) and extracted with 1 M NaOH (3×50 mL). The organic phase was dried over $MgSO_4$ and concentrated. The residue was purified by column chromatography on silica gel (CH_2Cl_2/MeOH/Et_3N = 95:5:0.5, R_f ~ 0.20). The amine was dissolved in MeOH (5 mL) and 1 mL of concentrated HCl was added. The solution was stirred at room temperature for 30 minutes before 10 mL of water and 1 mL of NH_4PF_6 solution (100 mg/mL) were added. After stirring for one hour, the mixture was extracted with DCM (3×50 mL). The organic phase was dried over $MgSO_4$ and concentrated by rotary evaporation. The title compound was obtained as a yellow solid (23 mg, 72% over two steps).

^{1}H NMR (700 MHz, CD_3CN, 298 K): 7.91 (s, H_j, 2H), 7.85-7.82 (m, H_b, 2H), 7.62-7.59 (m, H_c, 2H), 7.50 (t, *J* = 1.9 Hz, H_m, 1H), 7.26 (d, *J* = 1.8 Hz, H_l, 2H), 7.14-7.07 (br, NH_2, 2H), 6.95 (d, *J* = 8.3 Hz, H_3, 1H), 6.92 (d, *J* = 2.0 Hz, H_1, 1H), 6.81 (dd, *J* = 8.3 and 2.0 Hz, H_2, 1H), 5.58, (s, H_k, 2H), 5.22 (s, H_e, 2H), 4.22 (t, *J* = 6.2 Hz, H_a, 2H), 4.15-4.11 (m, H_4, 4H), 3.86-3.83 (m, H_5, 4H), 3.68k-3.65 (m, H_6, 4H), 3.61-3.60 (m, H_7, 4H), 3.59-3.57 (m, H_8 and H_9, 8H), 3.12-3.08 (m, H_f, 2H), 2.82-2.78 (m, H_i, 2H), 2.61 (s, H_d, 3H), 2.45 (s, $H_{d'}$, 3H), 1.78-1.74 (m, H_g and H_h, 4H), 1.30 (s, H_n, 18H) ppm.

^{13}C NMR (176 MHz, CD_3CN, 298 K): δ = 155.15, 152.87, 148.99, 148.59, 146.21, 142.87, 141.64, 136.14, 134.14, 132.57, 132.12, 130.55, 125.56, 124.21, 124.07, 123.04, 121.42, 113.69, 113.18, 70.68, 70.50, 70.43, 70.20, 70.14, 70.11, 68.39, 56.91, 53.11, 52.17, 48.12, 35.61, 31.55, 25.76, 25.71, 23.72, 14.25, 10.30 ppm.
ESI-MS (*m*/*z*): calculated for $[C_{52}H_{74}N_8O_7K]^+$: 961.5312, found 961.5298.

3. Additional NMR experiments

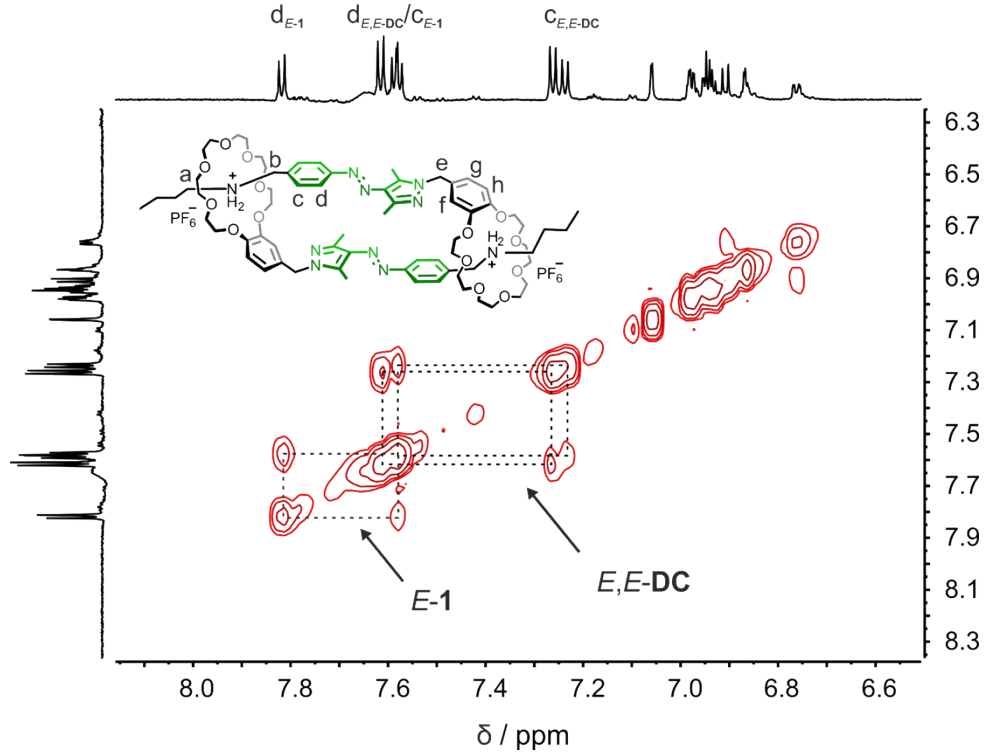

Fig. S1 Partial ^{1}H-^{1}H COSY spectrum of *E*-**1** in CD_3CN (700 MHz, 10 mM, 298 K).

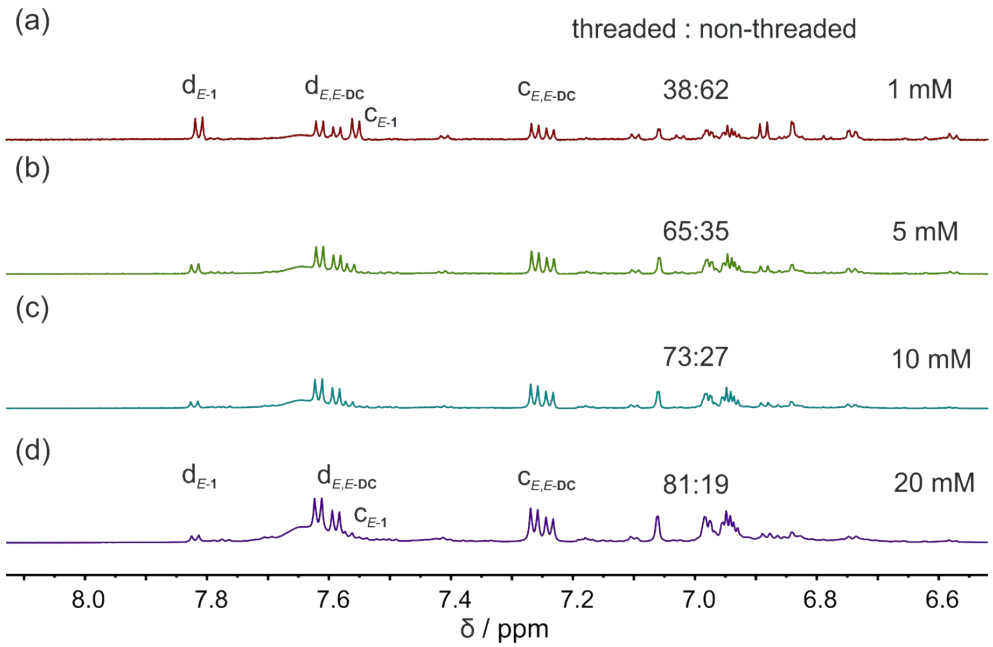

Fig. S2 Partial ^{1}H NMR spectra of **1** in CD_3CN at the concentrations of (a) 1 mM, (b) 5 mM, (c) 10 mM and (d) 20 mM (700 MHz, 298 K). Non-threaded *E*-monomer: *E*-**1**; and threaded *E*-dimer: *E*,*E*-**DC**.

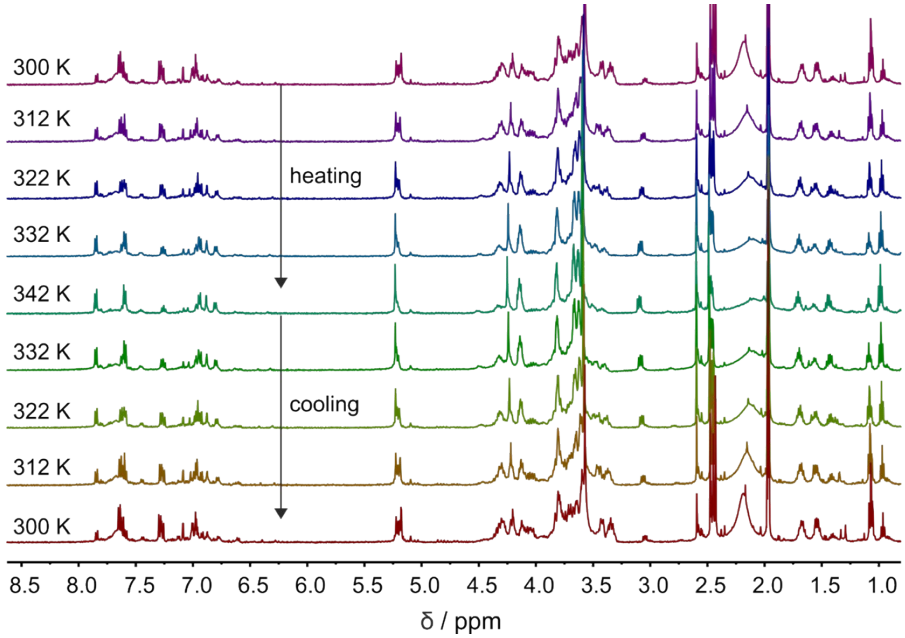

Fig. S3 VT-NMR experiment of **1** (10 mM in CD_3CN) upon heating and cooling. The characteristic signals for *E*,*E*-**DC** and diastereotopic splitting diminished at elevated temperatures and were retrieved after cooling down to 300 K.

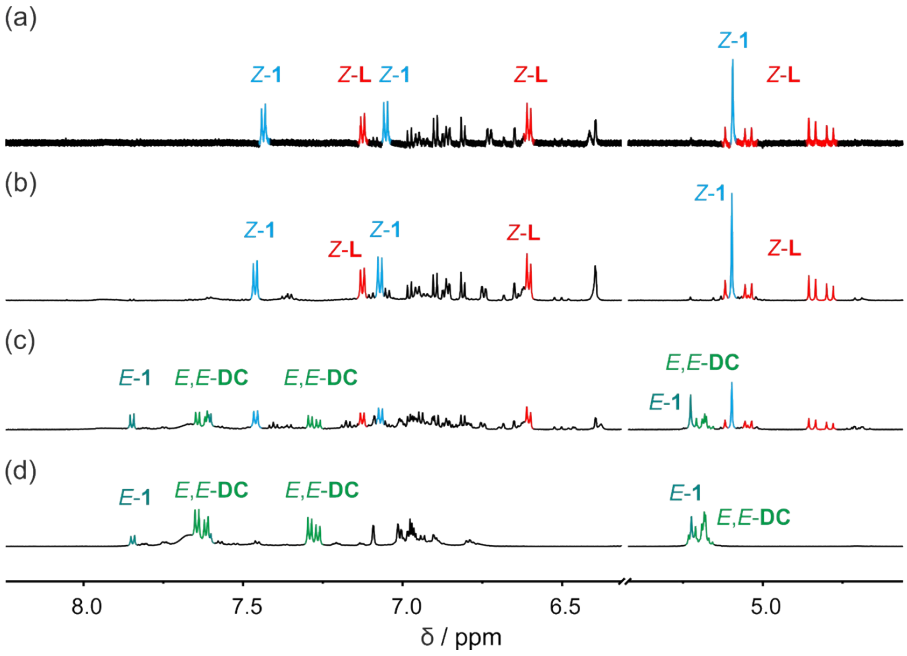

Fig. S4 Partial ^{1}H NMR spectra of *Z*-**1** in CD_3CN at the concentrations of (a) 1 mM, (b) 5 mM, (c) 10 mM and (d) 20 mM (700 MHz, 298 K). All spectra were recorded immediately after UV irradiation for 10 min. In (c) and (d), the appearance of *E*-**1** and *E*,*E*-**DC** is the result of increasing protonation followed by thermal backswitching. Non-threaded *E*-monomer: *E*-**1**; Non-threaded *Z*-monomer: *Z*-**1**; threaded *E*-dimer: *E*,*E*-**DC**; and threaded *Z*-monomer: *Z*-**L**.

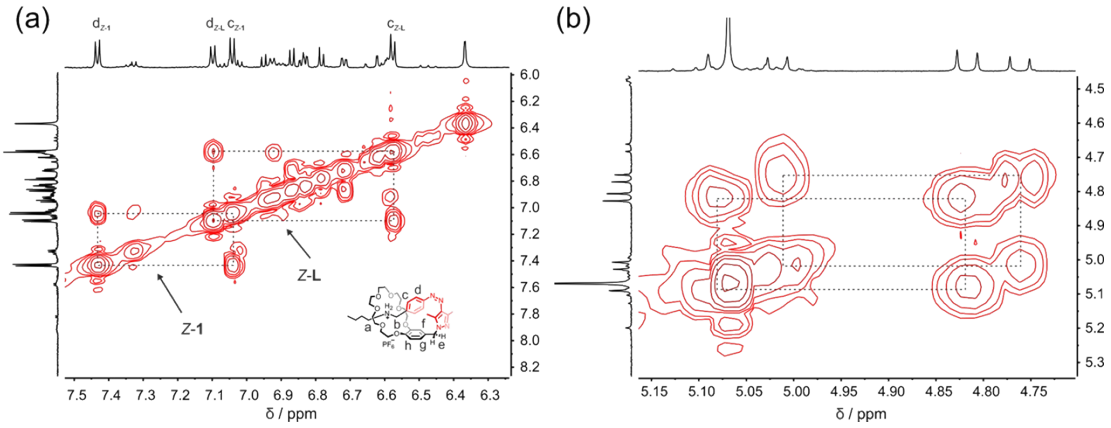

Fig. S5 Partial ^{1}H-^{1}H COSY spectrum of *Z*-**1** at (a) aromatic region and (b) the region of methylene protons H_e in CD_3CN (700 MHz, 5 mM, 298 K).

4. IMS experiments

In IMS experiments, the acetonitrile solutions, which were used in NMR experiments, were diluted with DCM for two reasons: On one hand, the much less competitive mixture slows down the building block exchange and thus reduces rearrangements in the MS sample solution to a minimum. On the other hand, the binding constant in the less competitive solvent mixture is higher and thus, the complexes survive even at mass spectrometric sample concentrations. These two aspects together make sure that the picture observed by mass spectrometry is as close as possible to the situation in the NMR experiments.

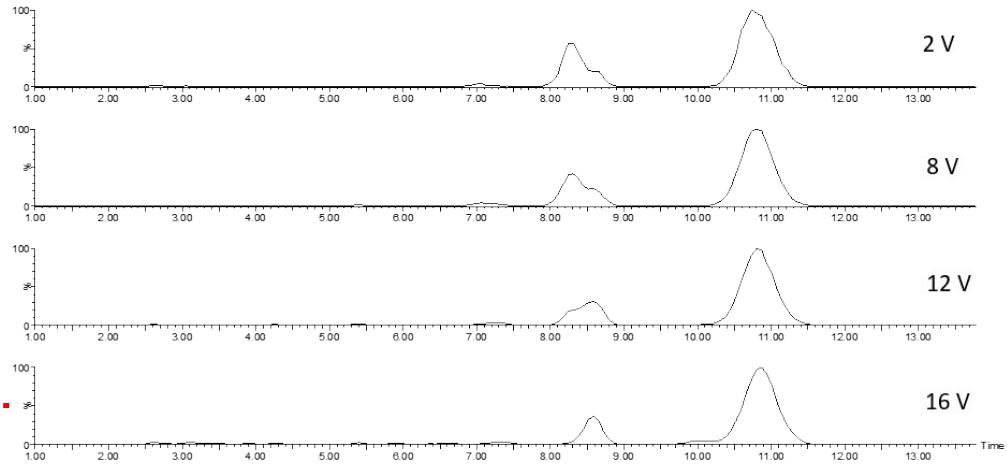

Fig. S6 Arrival-time distributions recorded in energy-resolved IMS experiments with mass-selected ions at *m*/*z* 654 after 5 min of UV irradiation. These experiments support the assignment of the peaks in the ATD to *E*,*Z*-**DC** (8.4 ms), *E*,*E*-**DC** (8.9 ms) and *Z*-**L** (10.9 ms): The peak for partially switched and therefore somewhat strained *E*,*Z*-**DC** vanishes at around 16 V collision voltage, while the unstrained *E*,*E*-**DC** daisy chain and the switched Z-isomer survive as the more stable species. ATDs are given in milliseconds.

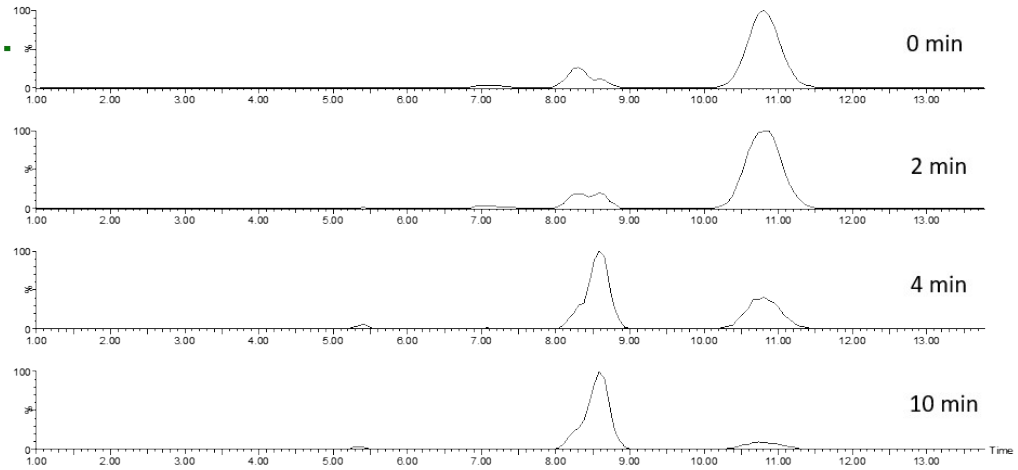

Fig. S7 ATDs of **1** under green light irradiation. At t = 0, the ATD was recorded with the sample after irradiating under 365 nm for 5 min. Clearly, the back-switching process occurs leading to the *E*,*E*-**DC** daisy chain. In contrast to the *E*-to-*Z* switching, the abundance of the *E*,*Z*-**DC** isomer does not change significantly indicating that the major fraction of the back-switched molecules undergo *Z*-to-*E* isomerization first and then directly assemble from two copies of *E*-**1**. ATDs are presented in milliseconds.

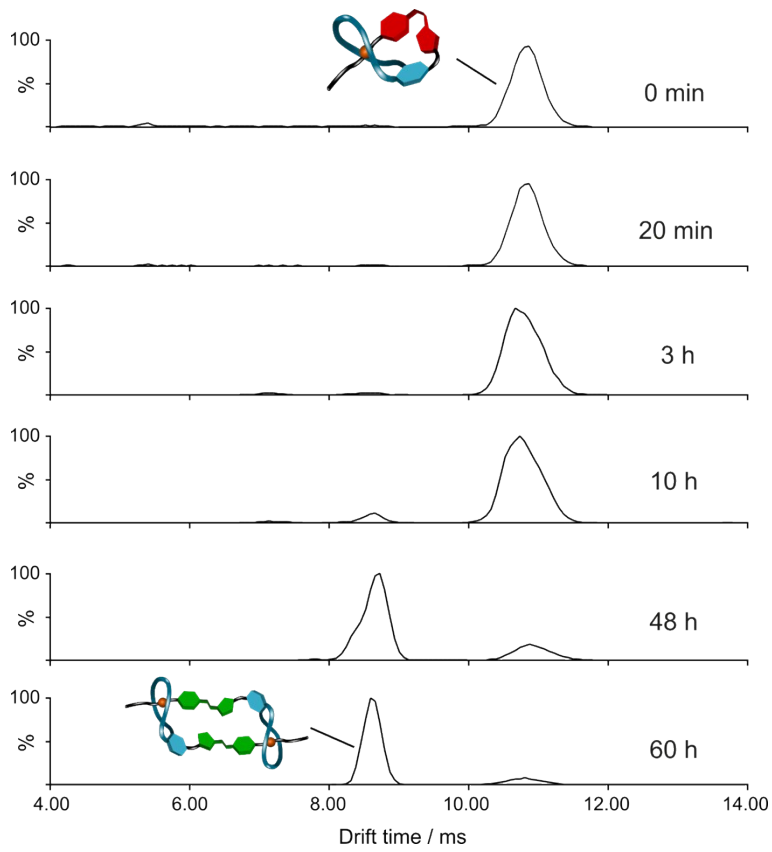

Fig. S8 Thermal stability of *Z*-**L** in the dark monitored by IMS. In the first 10 h, *Z*-**L** remains as major product. Over time, a dimer peak became visible due to *Z*-to-*E* back isomerisation of **1** and thus, the formation of *E*,*E*-**DC**. After 48 h, an intermediate *E*,*Z*-**DC** was clearly observed. Compared to the light-induced *Z*-to-*E* switching (Fig. S7), *E*,*Z*-**DC** is prominent here due to a slower process of the thermal-induced *Z*-to-*E* switching, so that the daisy chain assembly can compete. There is an intermediate stage, where about 50% of the compound is *E*-state and 50% is *Z*-state, so the assembly of *E*,*Z*-**DC** is expected. After 60 h in the dark, *E*,*E*-**DC** was recovered as the major product.

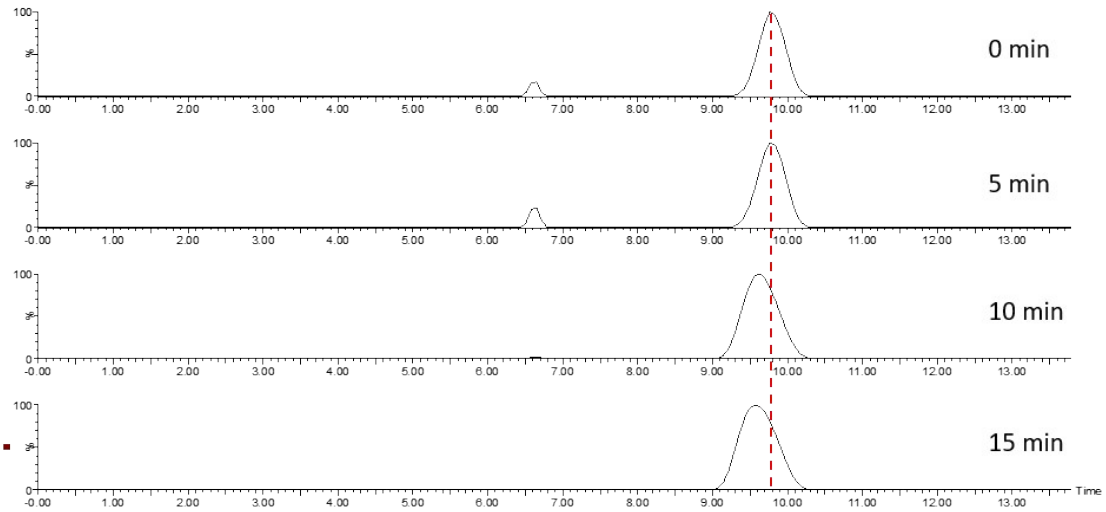

Fig. S9 ATDs of **2** under UV irradiation. The distribution shifted towards shorter drift time under UV irradiation, representing a photoswitching from *E*-**2** to *Z*-**2**. ATDs are presented in milliseconds.

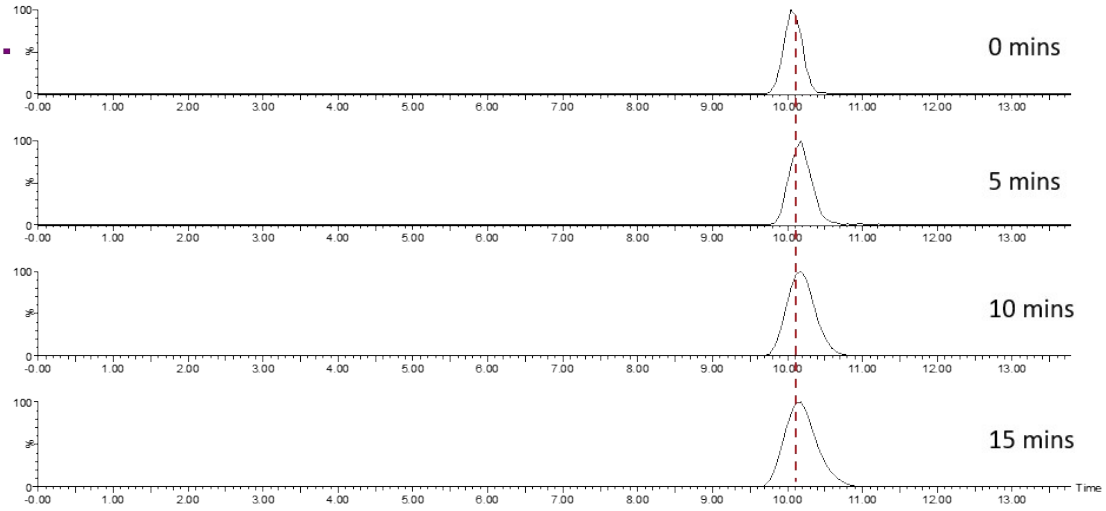

Fig. S10 ATDs of Boc-protected **2** under UV irradiation. Here, the distribution did not show a distinct difference in size due to a fast *Z*-*E* switching induced by protonation of azo nitrogen adjacent to the phenyl ring. ATDs are presented in milliseconds.

5. Computational Modelling and theoretical CCS values.

To support the assignment of the switching processes, computational modelling at the PM6 level was performed for *E*,*E*-**DC** (**Fig. S11**), *E*,*Z*-**DC** (**Fig. S12**), threaded monomer *Z*-**L** (**Fig. S13**), non-threaded monomer *Z*-**1** (**Fig. S14**), and *E*-**1** (**Fig. S15**). The respective structures were initially constructed to allow the maximum number of hydrogen bonds between crown ether and axle and to maximise the conjugation of the azo groups with the adjacent aromatic rings followed by optimisation at the PM6 level. These structures were then used to perform the theoretical CCS calculations (**Table S1**) which can be used to rationalise the proposed pathway.

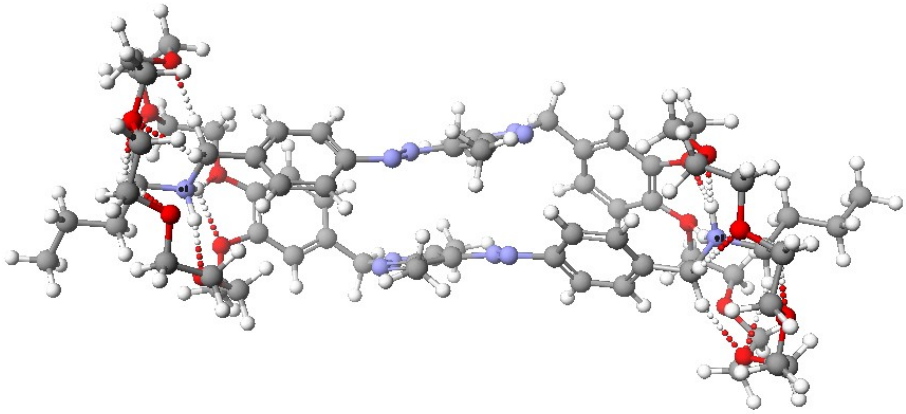

Fig. S11 PM6 optimised structure of *E*,*E*-**DC**. Hydrogen bonds are denoted by the dotted bonds.

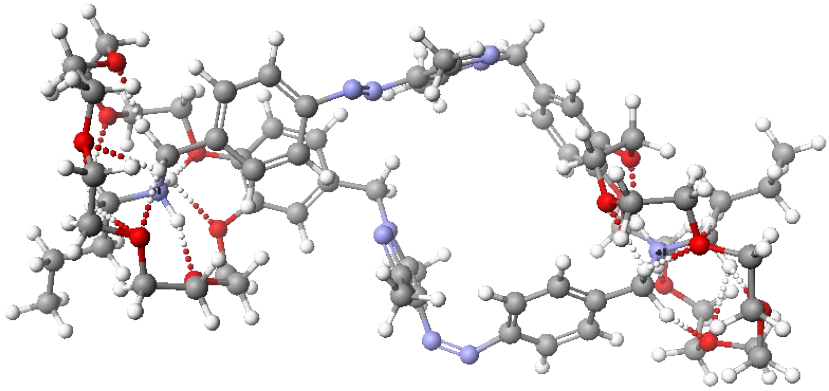

Fig. S12 PM6 optimised structure of *E*,*Z*-**DC**. Hydrogen bonds are denoted by the dotted bonds.

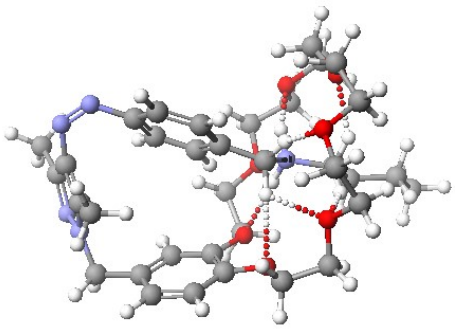

Fig. S13 PM6 optimised structure of threaded *Z*-**L**. Hydrogen bonds are denoted by the dotted bonds.

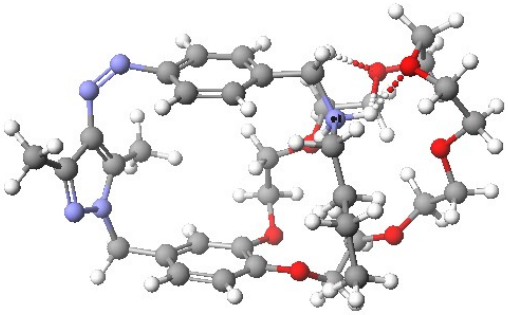

Fig. S14 PM6 optimised structure of non-threaded *Z*-**1**. Hydrogen bonds are denoted by the dotted bonds.

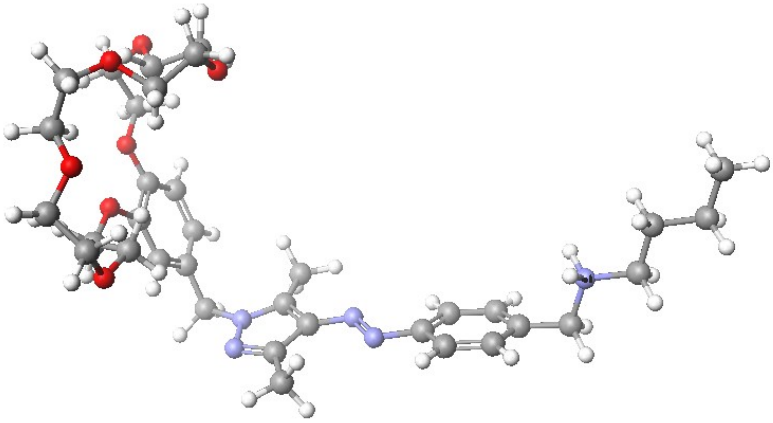

Fig. S15 PM6 optimised structure of *E*-**1** (non-threaded).

Table S1: Calculated heat of formations and theoretical CCS values of the different optimised structures.

conformation	**heat of formation** (kJ mol^{-1})	$^{TM}CCS_{N_2}$ (Å^2)
E,*E*-**DC**	-600.5	467
E,*Z*-**DC**	-616.5	462
Z-**L** (threaded)	-327.0	278
Z-**1** (non-threaded)	-310.2	267
E-**1**	-223.3	331

E,*Z*-**DC** having a more favourable value in energy than the *E*,*E*-**DC** can explain the ready *E*,*E*-**DC** to *E*,*Z*-**DC** switching which is observed under UV irradiation. When considering the monomer which would form, the threaded *Z*-**L** is more stable than the non-threaded *Z*-**1** and will thus be expected to predominate between the two conformations. The heat of formation difference (16.8 kJ/mol) between the two though is not large enough that it would prevent the necessary dethreading seen in the back switching process. In contrast, *E*-**1** does not benefit from any H-bonding observed for the other conformations and hence has a much less favourable heat of formation of (-223.3 kJ/mol). Dimerization of *E*-**1** to *E*,*E*-**DC** would be accompanied by a binding energy of 153.9 kJ/mol. Although this is a gas-phase calculation which amplifies the benefit of non-covalent interaction as compared to solution, this clearly rationalises the driving force for dimerization which is seen by IMS. Finally, the $^{TM}CCS_{N_2}$ are also in alignment with the proposed pathway with the initial *E*,*E*-**DC** switching to form the smaller *E*,*Z*-**DC** before finally disassembling to form the monomer. Our calculations are gas-phase calculations in the absence of counterions and thus may be somewhat limited with respect to conclusions that can be drawn for the situation in solution. However, counterion effects as well as solvent effects on the crown ether/ammonium binding pattern likely affect the binding in a similar manner for all threaded complexes. Therefore, our calculations support our interpretation of the NMR spectroscopic and IMS data.

6. UV/vis experiments

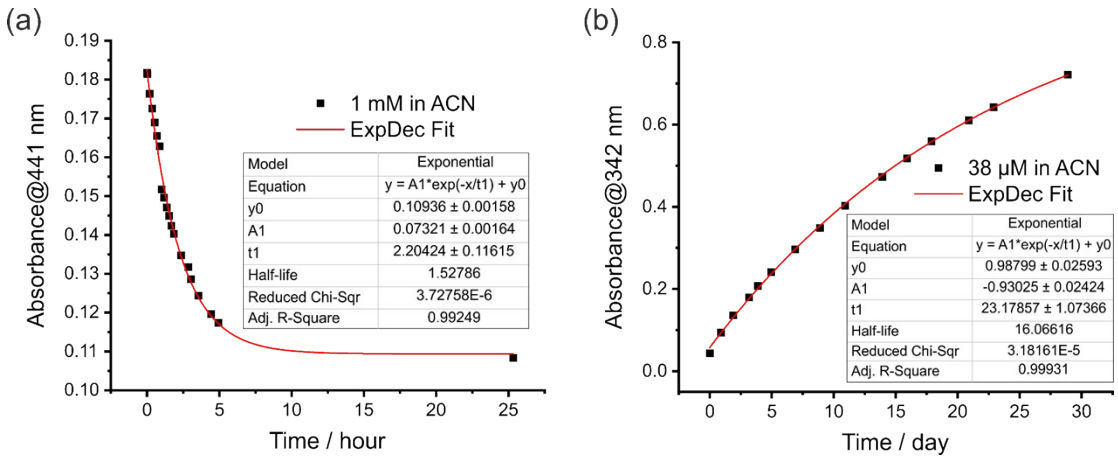

Fig. S16 Half-lives of *Z*-**1** at concentrations of (a) 1 mM ($t_{1/2}$ = 1.5 h) and (b) 38 μM ($t_{1/2}$ = 16 days) in CH_3CN in the dark. At t = 0, the spectra were recorded with the samples right after irradiating at 365 nm for 10 min. Absorbance at 441 nm is used to follow the back isomerisation to avoid the excessively high absorbance at 342 nm at the concentration of 1 mM.

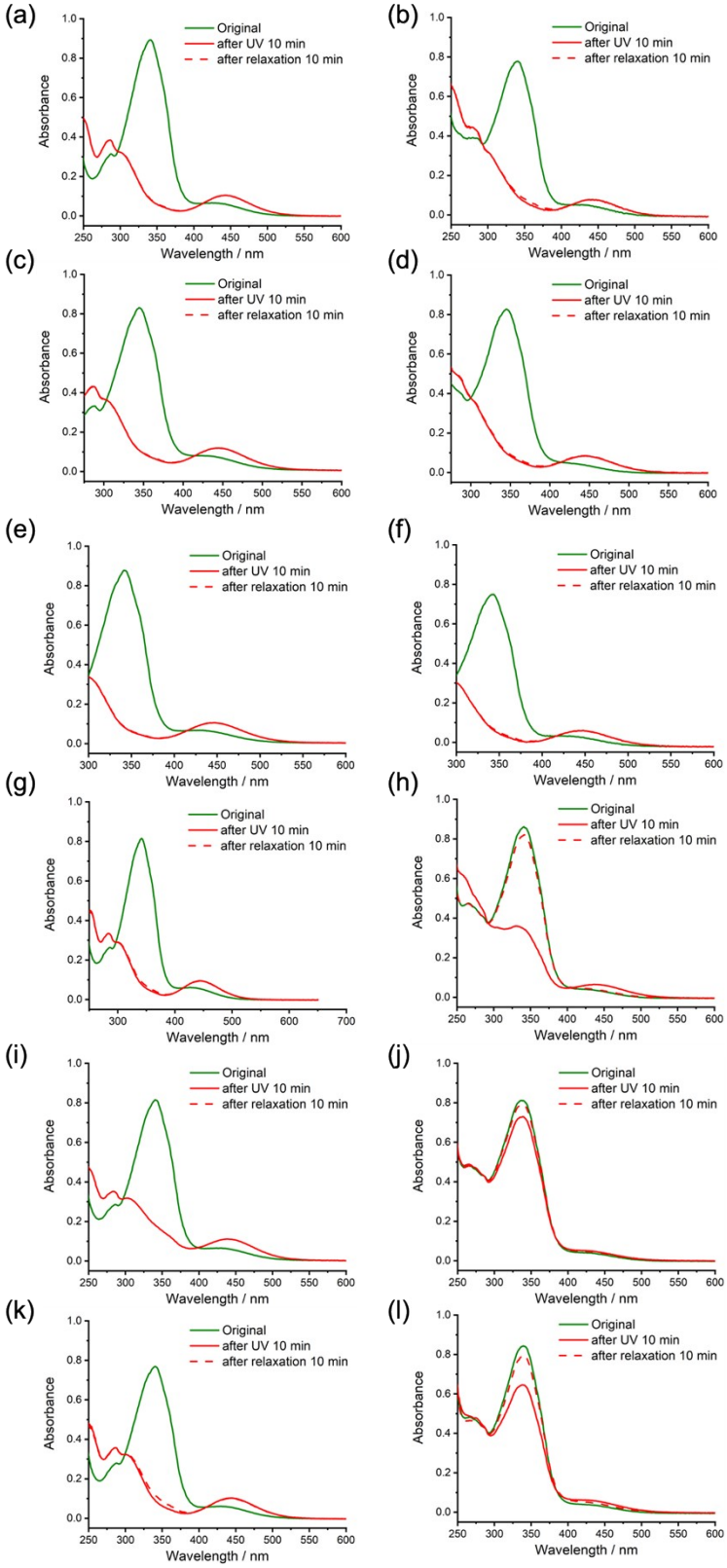

Fig. S17 UV/Vis spectra of Boc-protected **2** (left) and **2** (right) in CH_3CN (a, b), DMSO (c, d), THF (e, f), DCE (g, h), CH_2Cl_2 (i, j), $CHCl_3$ (k, l).

7. NMR spectra

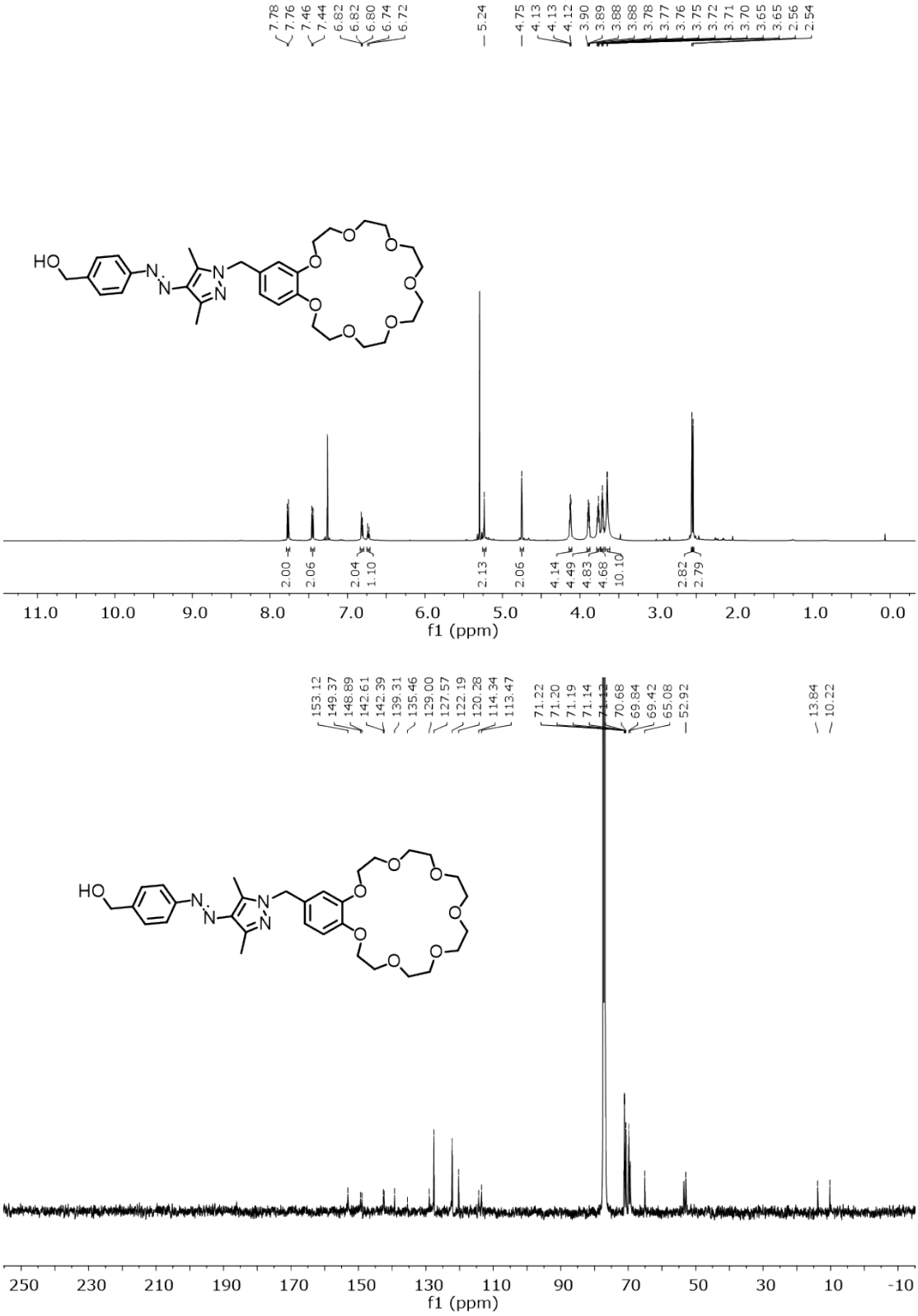

Fig. S18 ^{1}H (top) and ^{13}C (bottom) NMR spectrum (500/126 MHz, $CDCl_3$, 298 K) of **S3**.

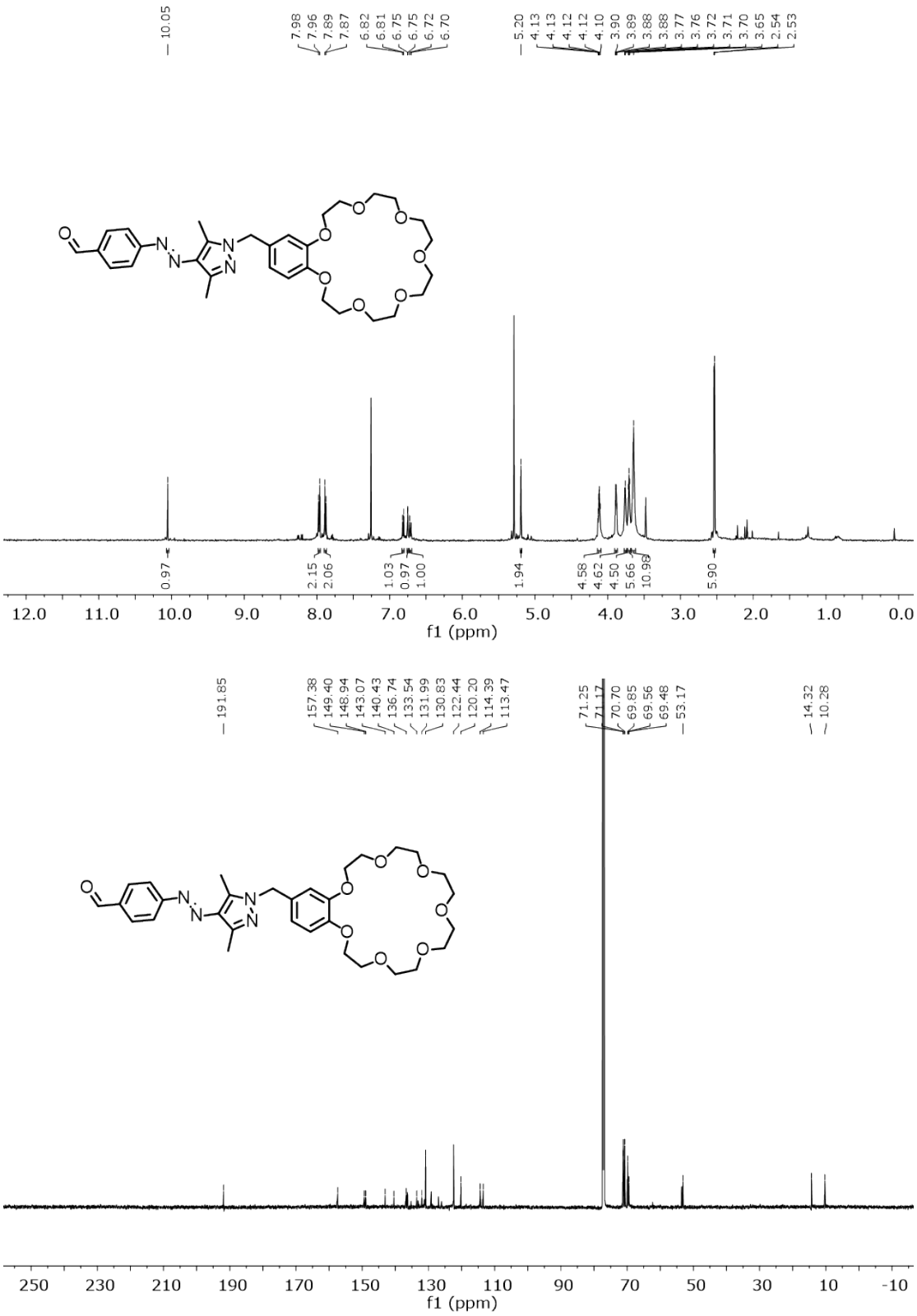

Fig. S19 ^{1}H (top) and ^{13}C (bottom) NMR spectrum (700/176 MHz, $CDCl_3$, 298 K) of **S4**.

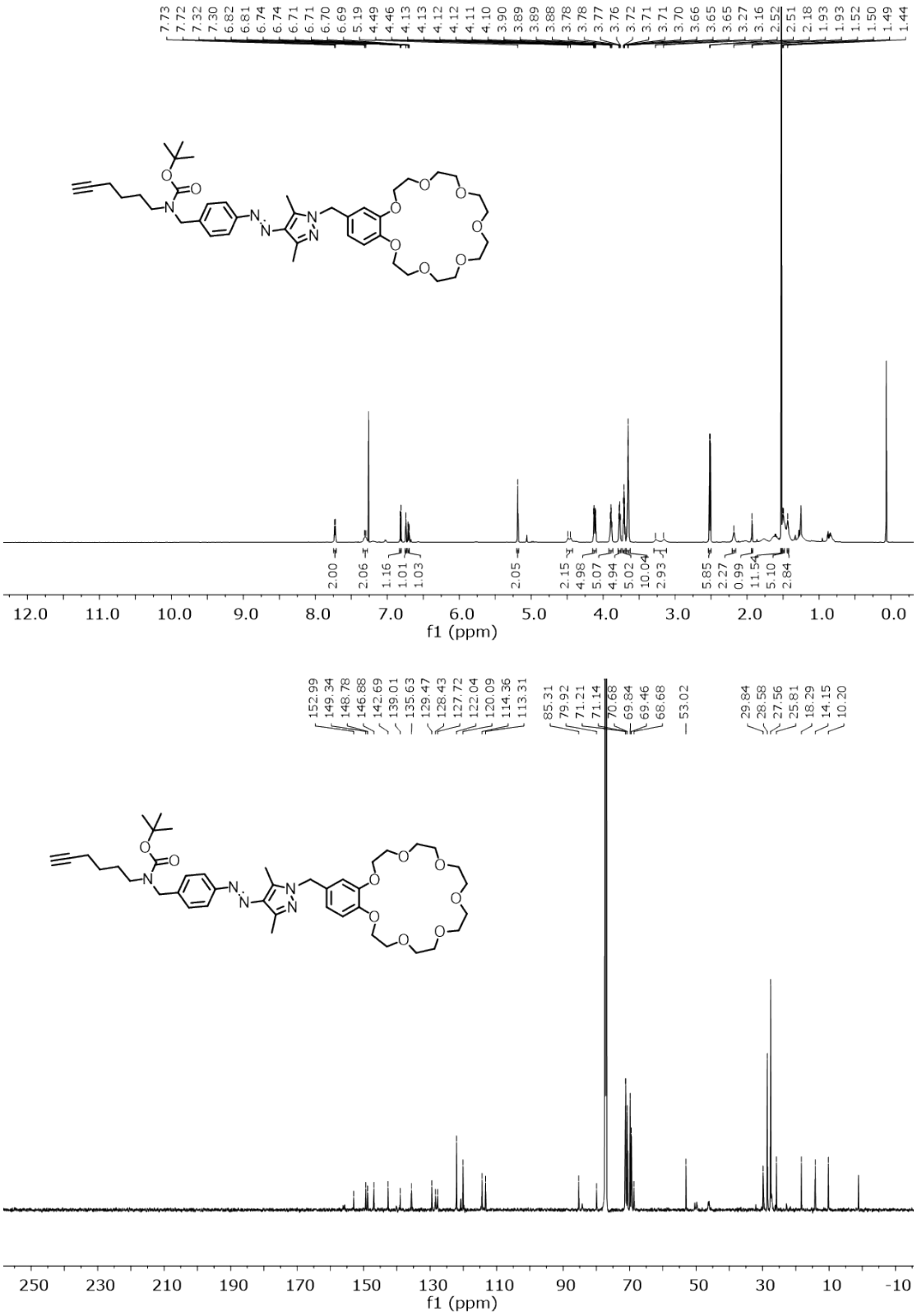

Fig. S20 ^{1}H (top) and ^{13}C (bottom) NMR spectrum (700/176 MHz, $CDCl_3$, 298 K) of **S6**.

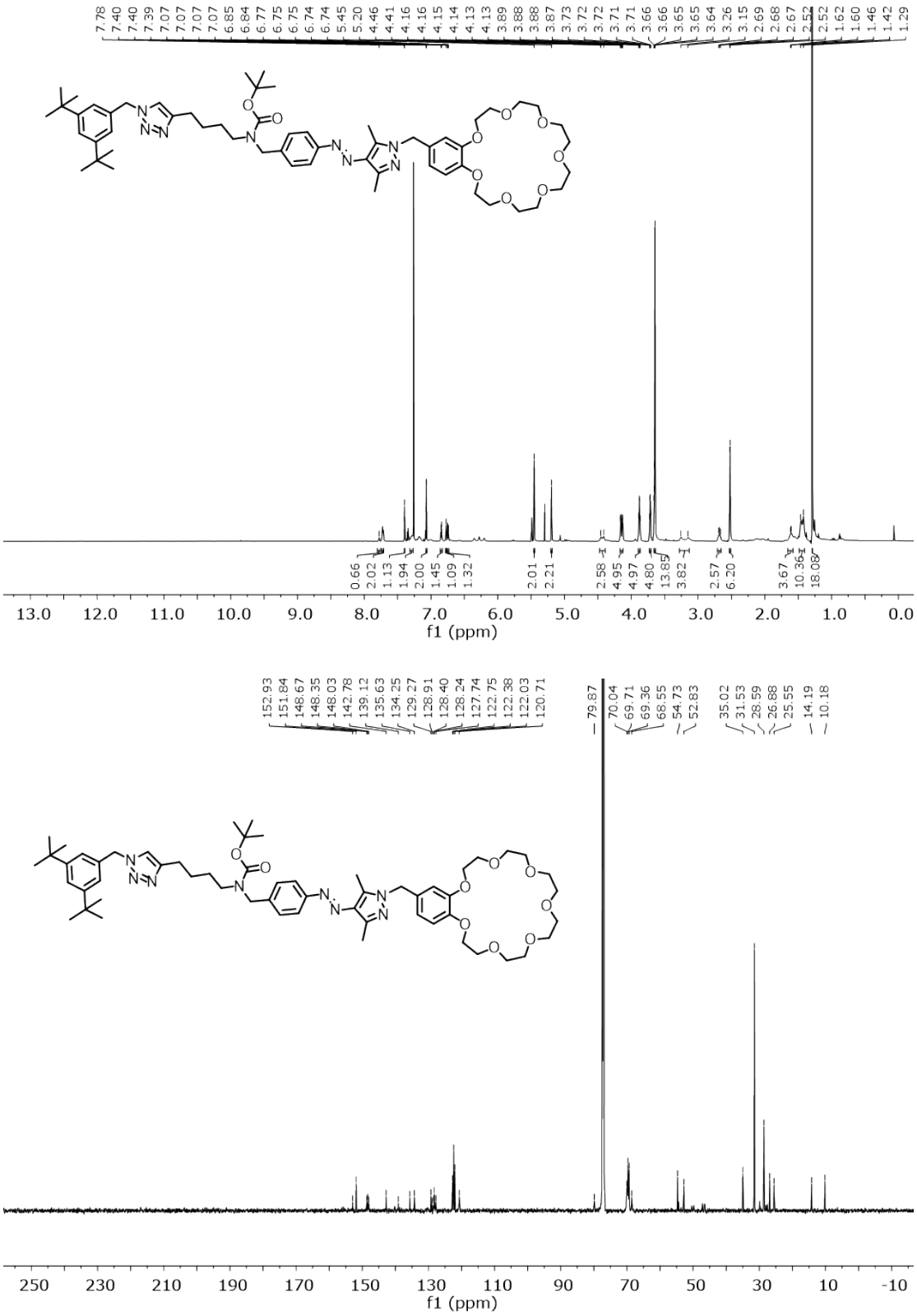

Fig. S21 ^{1}H (top) and ^{13}C (bottom) NMR spectrum (700/176 MHz, $CDCl_3$, 298 K) of **S8**.

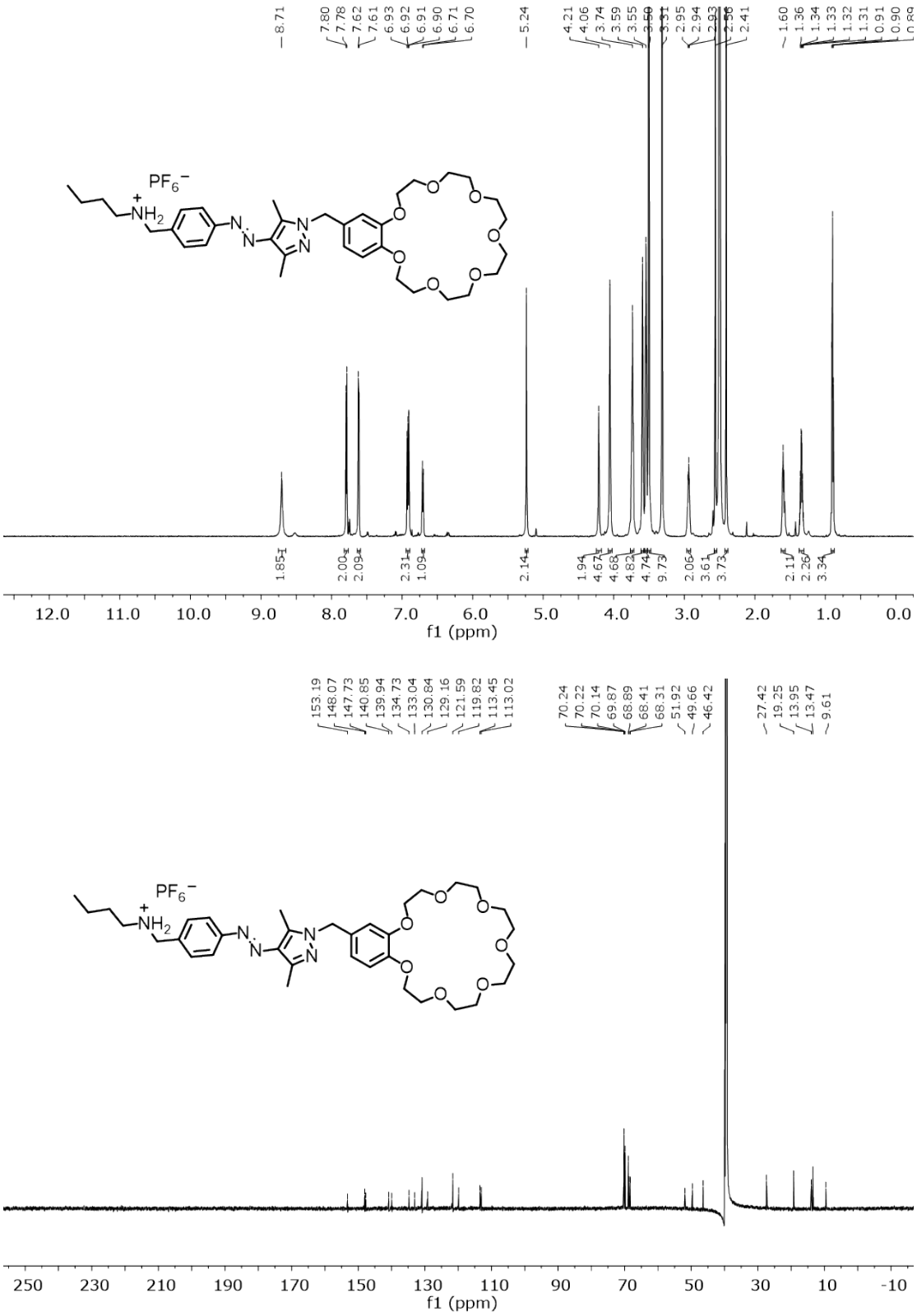

Fig. S22 ^{1}H (top) and ^{13}C (bottom) NMR spectrum (700/176 MHz, DMSO-d_6, 298 K) of thread **1**.

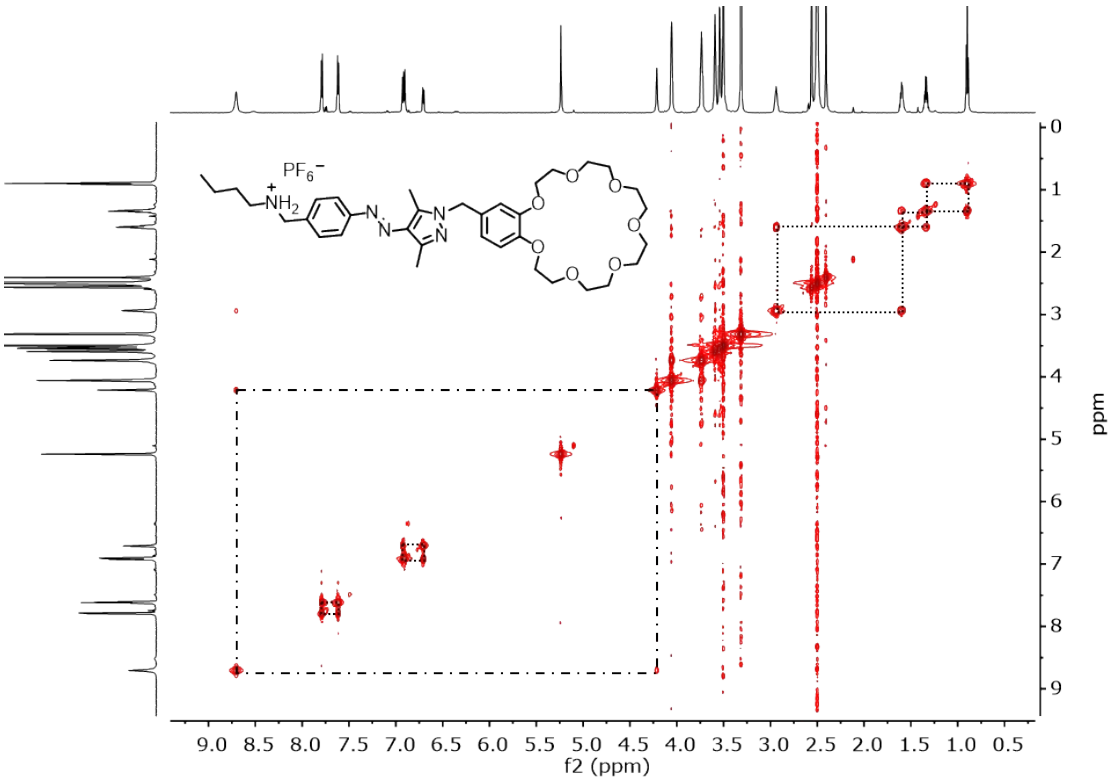

Fig. S23 COSY spectrum (700 MHz, DMSO-d_6, 298 K) of thread **1**.

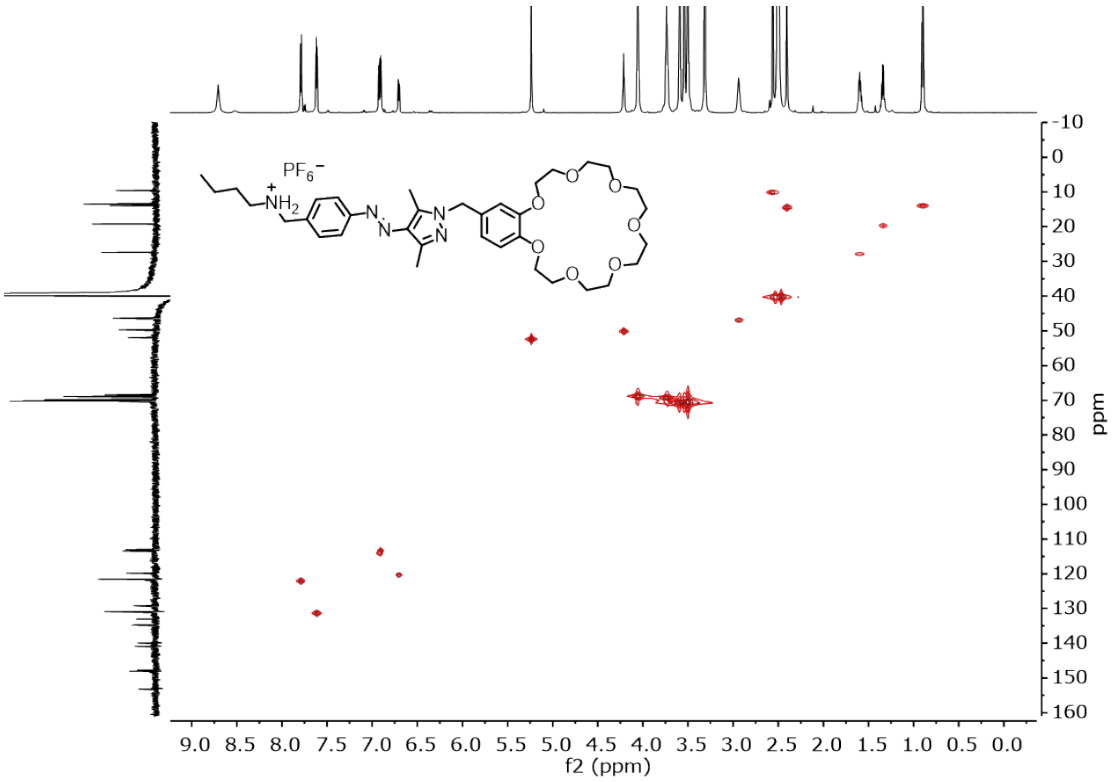

Fig. S24 HMQC spectrum (700/176 MHz, DMSO-d_6, 298 K) of thread **1**.

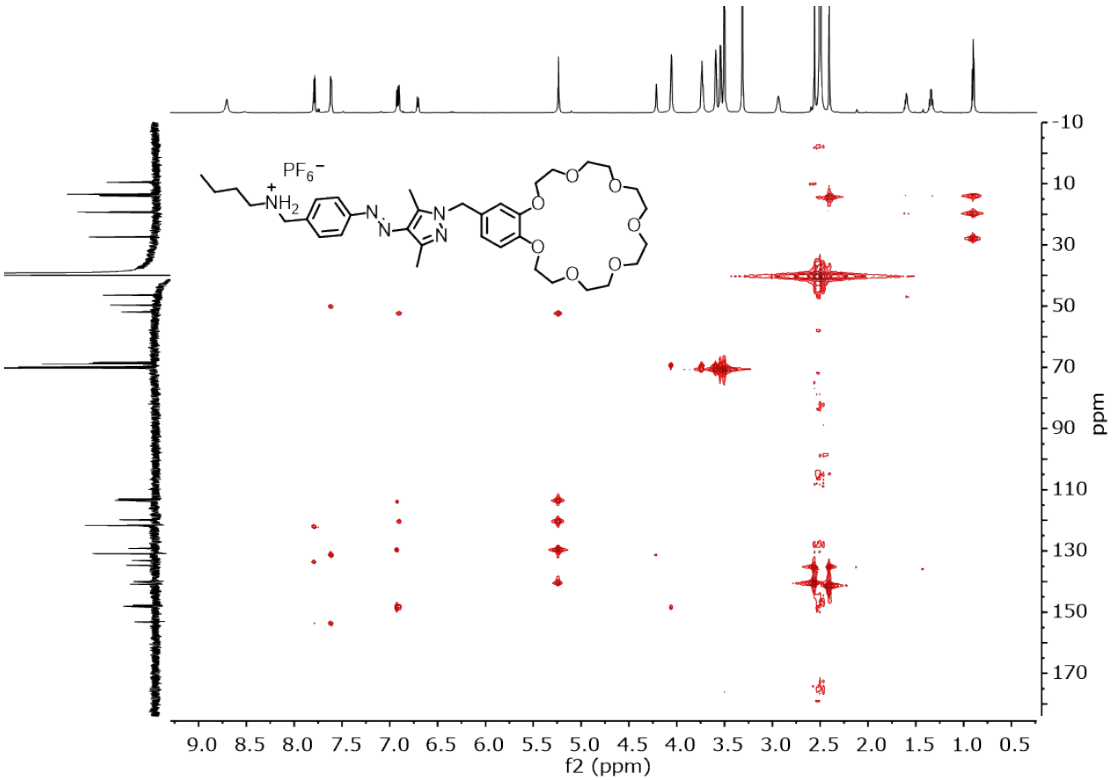

Fig. S25 HMBC spectrum (700/176 MHz, DMSO-d_6, 298 K) of thread **1**.

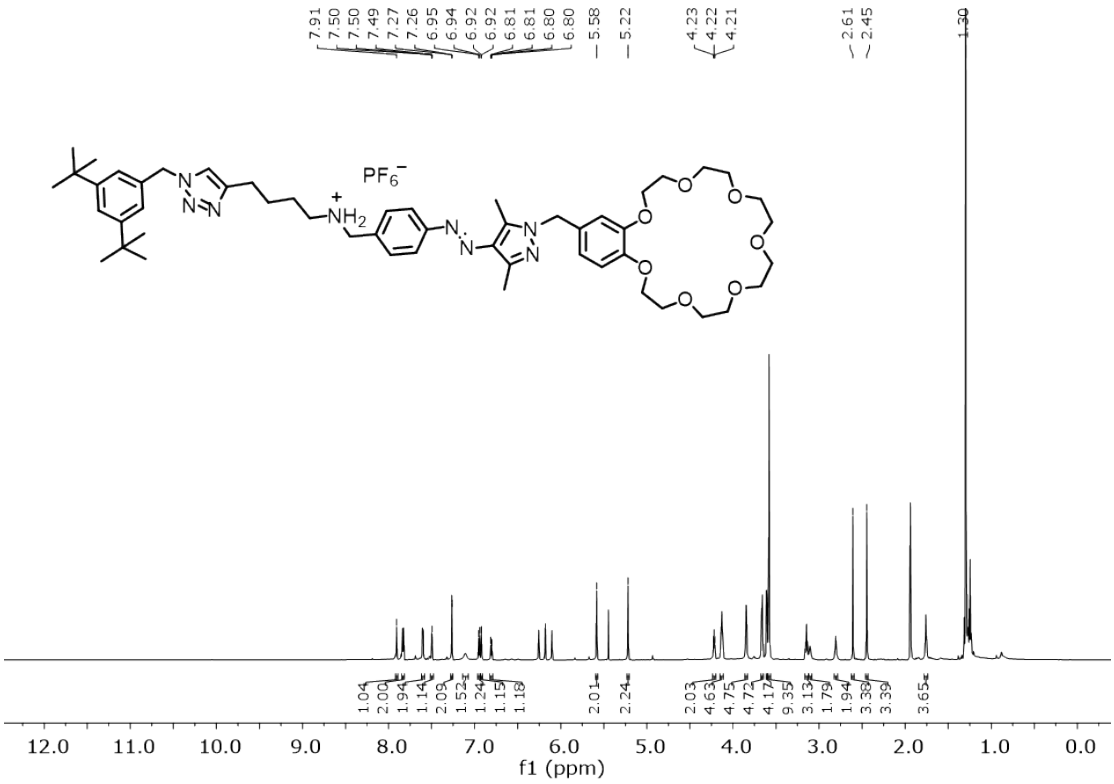

Fig. S26 ^{1}H NMR spectrum (700 MHz, CD_3CN, 298 K) of control compound **2**.

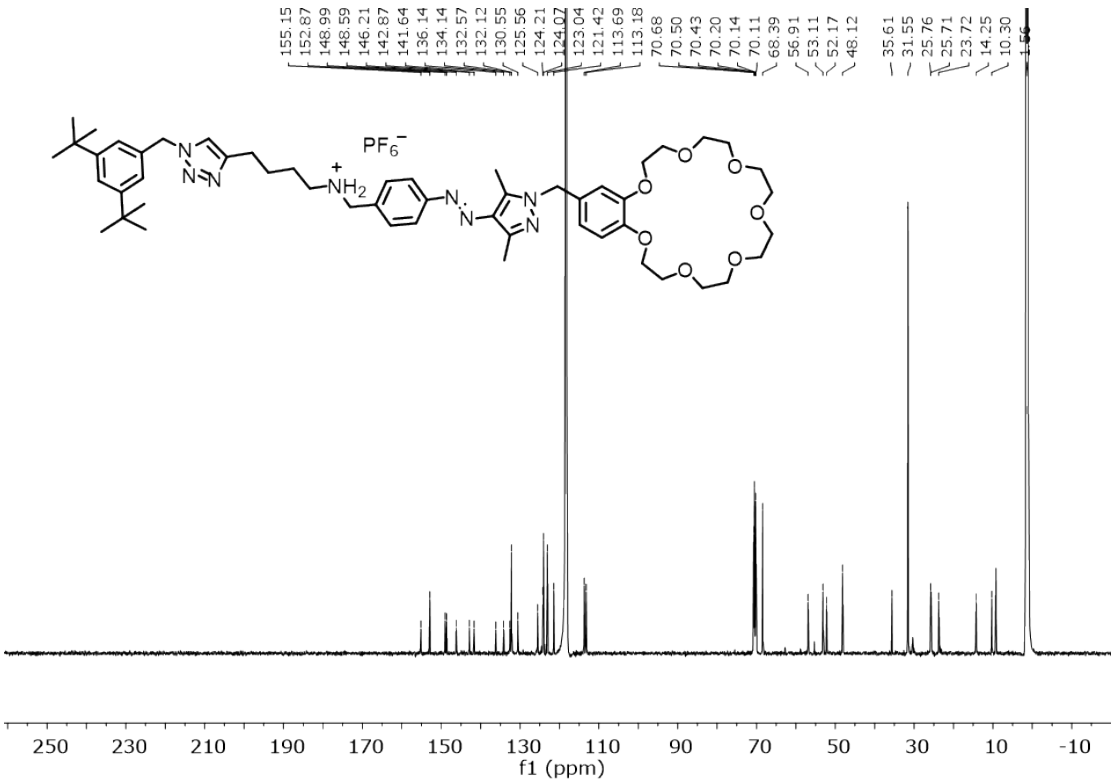

Fig. S27 ^{13}C NMR spectrum (176 MHz, CD_3CN, 298 K) of control compound **2**.

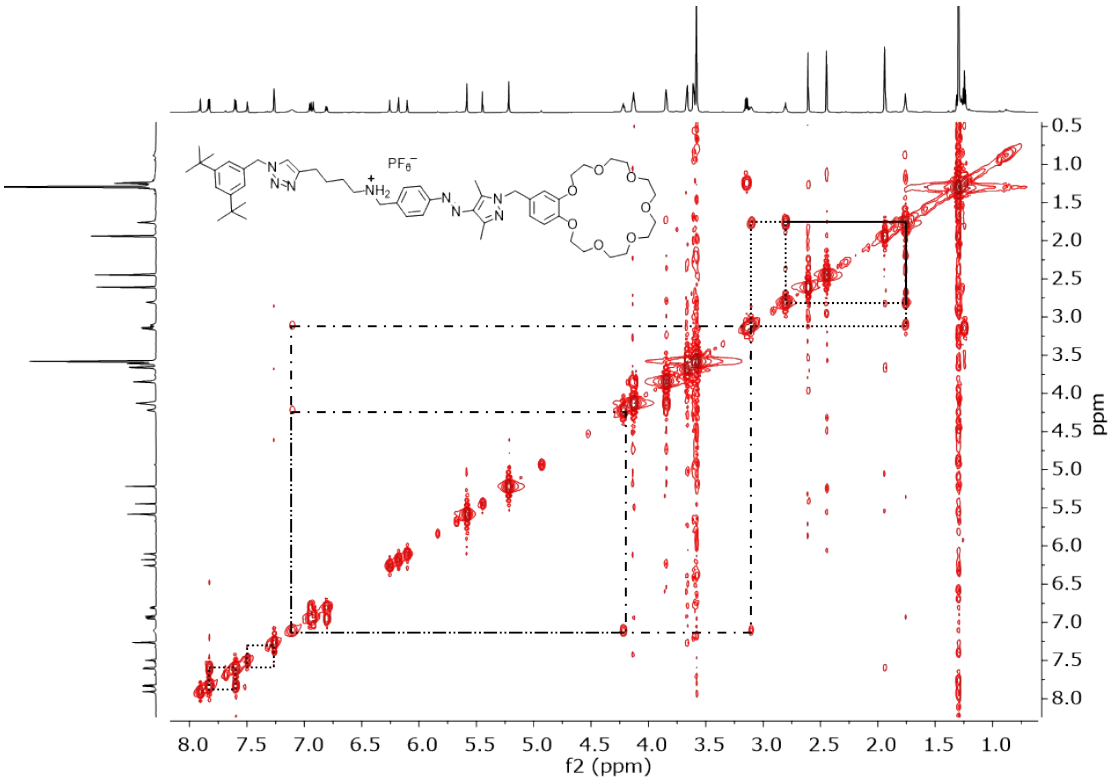

Fig. S28 COSY spectrum (700 MHz, CD_3CN, 298 K) of control compound **2**.

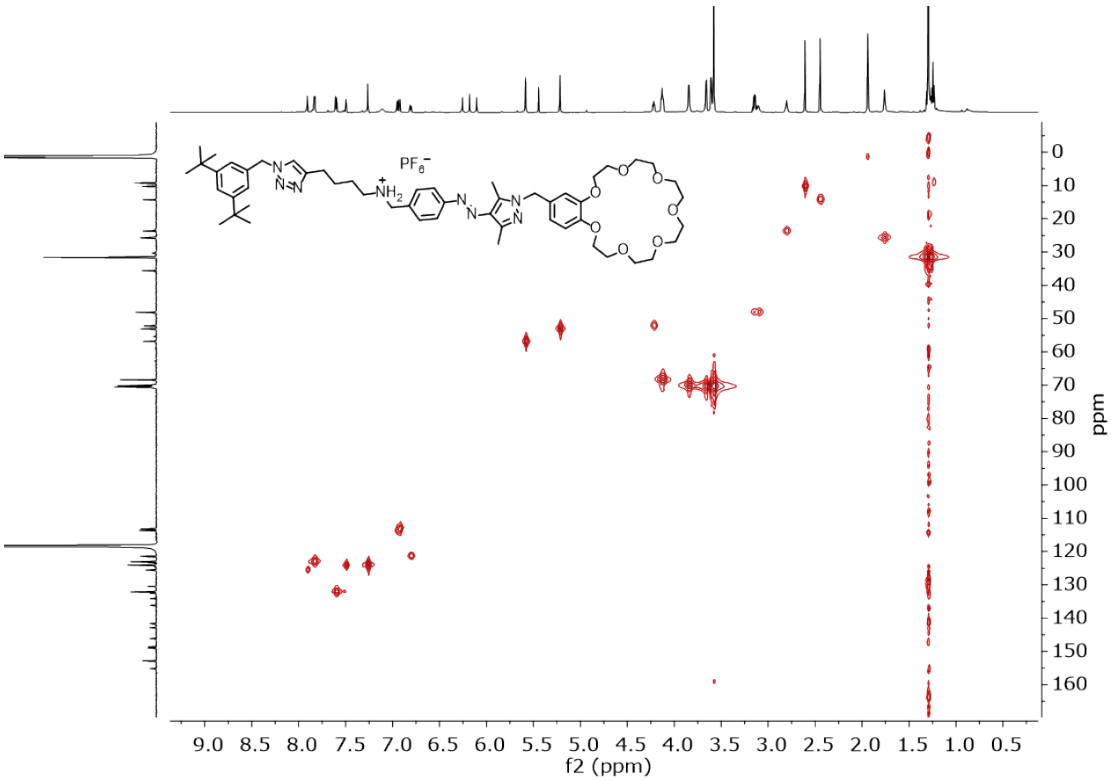

Fig. S29 HMQC spectrum (700/176 MHz, CD_3CN, 298 K) of control compound **2**.

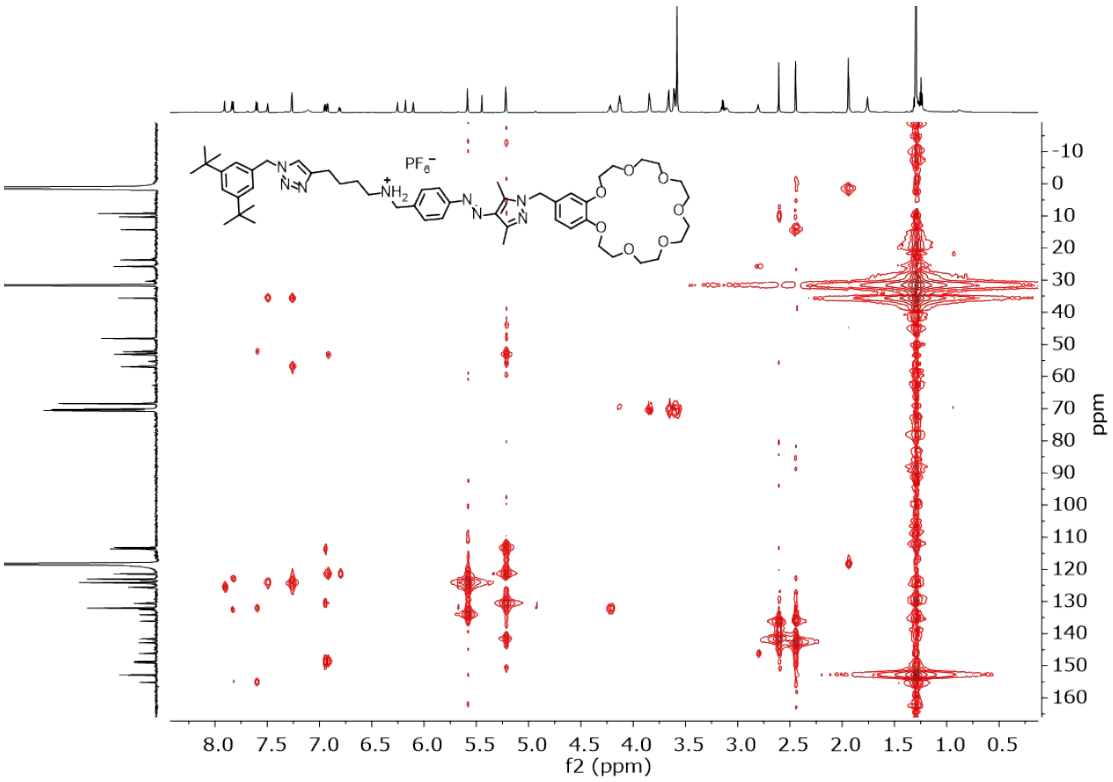

Fig. S30 HMBC spectrum (700/176 MHz, CD_3CN, 298 K) of control compound **2**.

8. ESI mass spectra

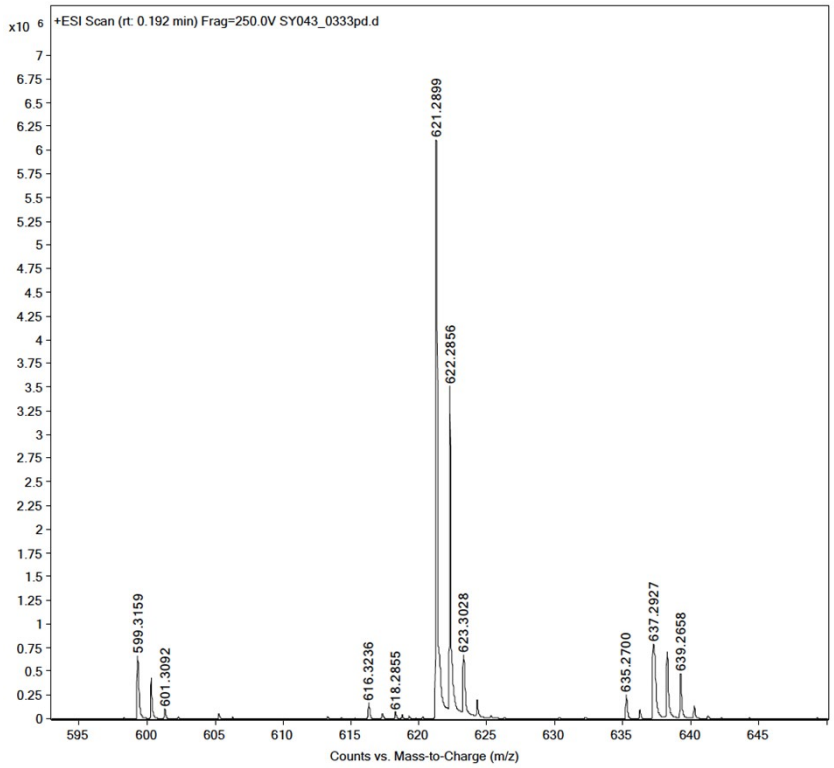

Fig. S31 ESI-MS of **S3**.

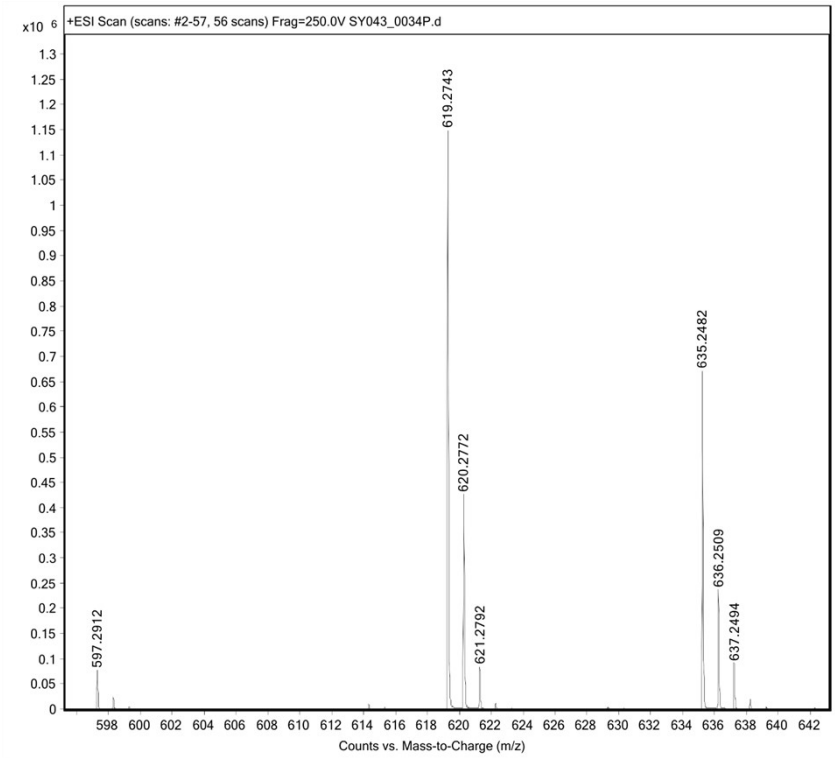

Fig. S32 ESI-MS of **S4**.

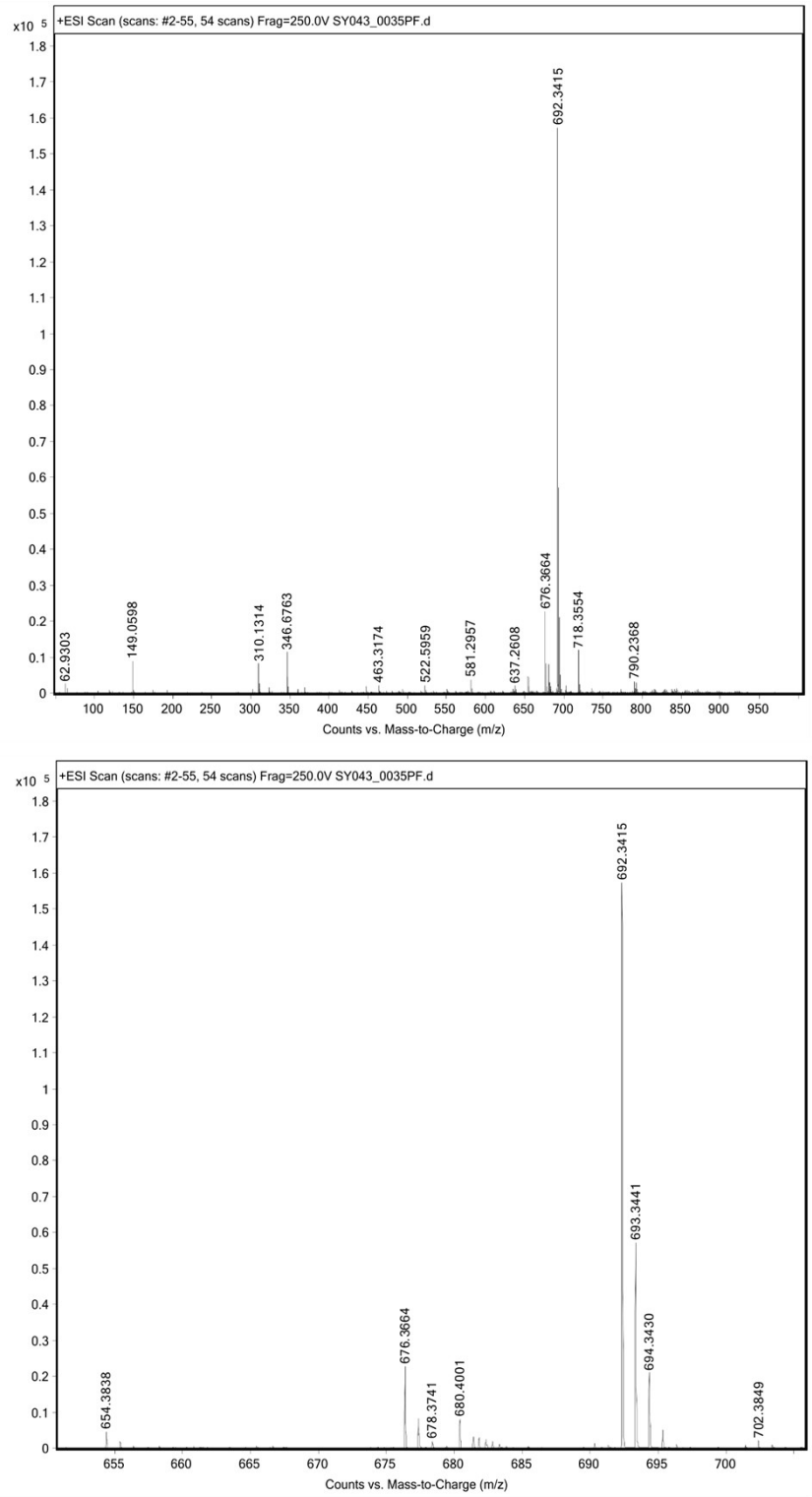

Fig. S33 ESI-MS of **1** (mostly [**1**-PF_6+K]$^+$). Full spectrum (top) and zoom-in (bottom).

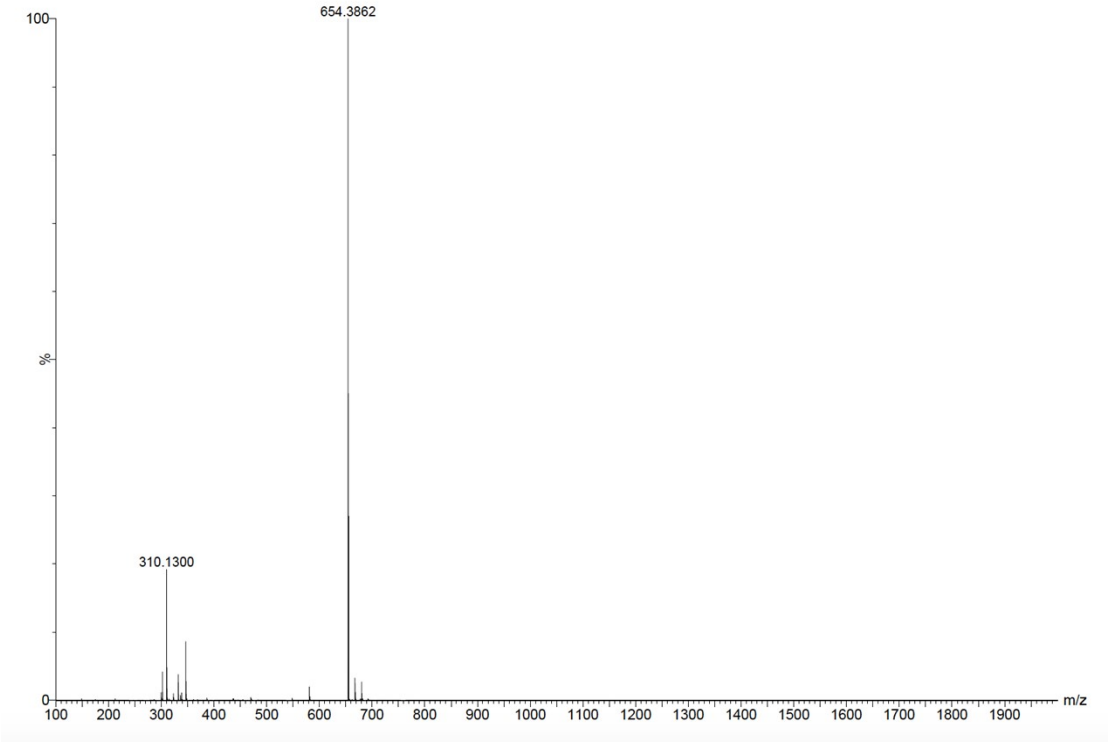

Fig. S34 Full, non-mass selected ESI-MS of **1** (mostly [**1**-PF_6]$^+$).

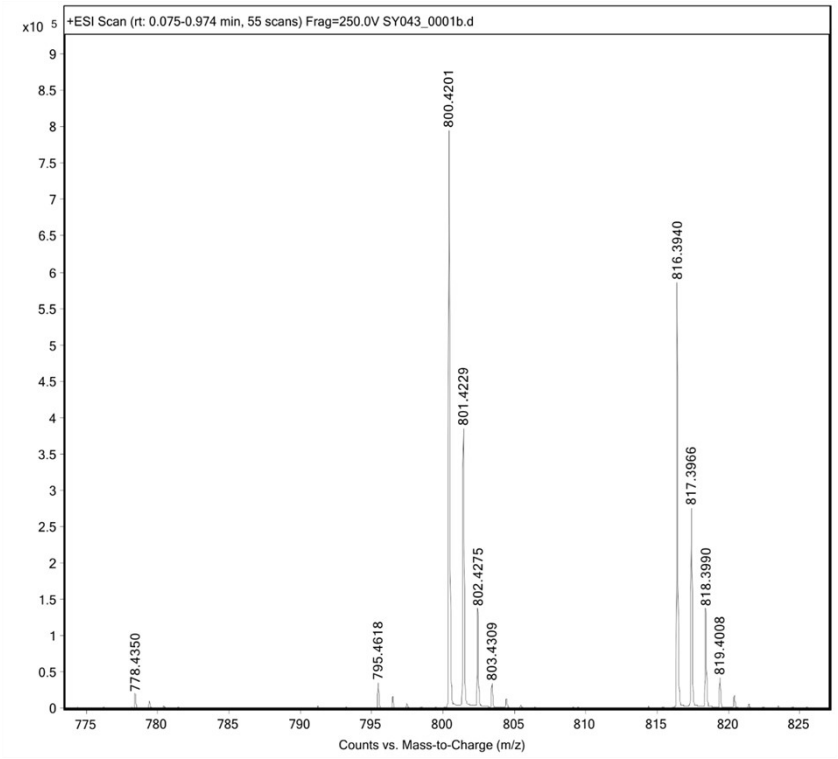

Fig. S35 ESI-MS of **S6**.

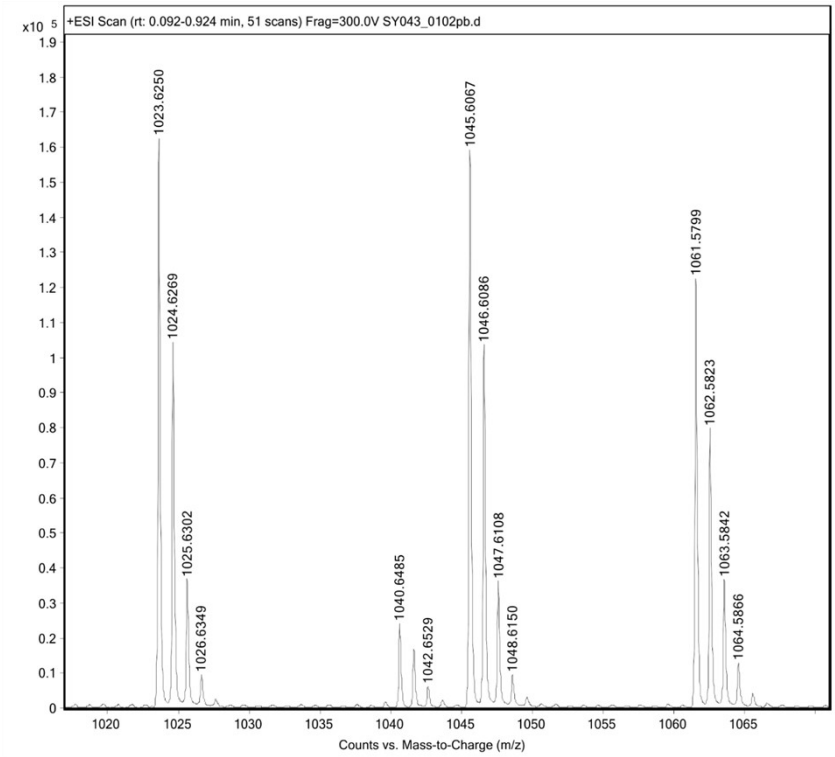

Fig. S36 ESI-MS of **S8**.

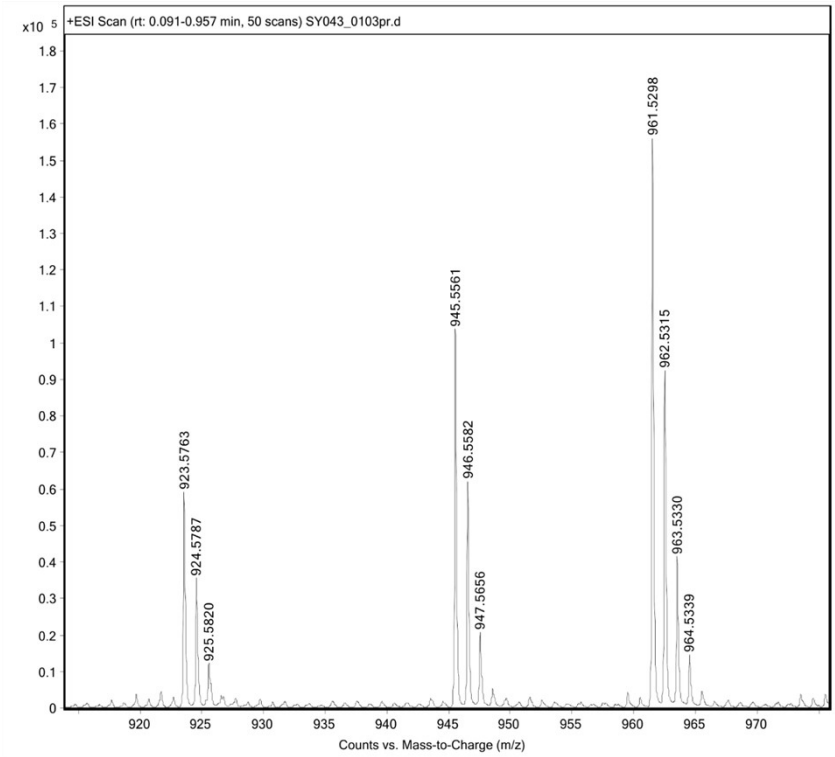

Fig. S37 ESI-MS of **2**.

9. References

S1. L. Chen, Y.-K. Tian, Y. Ding, Y.-J. Tian and F. Wang, *Macromolecules*, 2012, **45**, 8412.

S2. W. Wang, Y. Zhang, B. Sun, L.-J. Chen, X.-D. Xu, M. Wang, X. Li, Y. Yu, W. Jiang and H.-B. Yang, *Chem. Sci.*, 2014, **5**, 4554.

S3. C.-W. Chu, L. Stricker, T. M. Kirse, M. Hayduk and B. J. Ravoo, *Chem. Eur. J.*, 2019, **24**, 6131.

S4. J. Budhathoki-Uprety, J. F. Reuther and B. M. Novak, *Macromolecules*, 2012, **45**, 8155.

S5. J. J. Gassensmith, L. Barr, J. M. Baumes, A. Paek, A. Nguyen and B. D. Smith, *Org. Lett.*, 2008, **10**, 3343.